

Exoplanets

Lecture 10
MFF UK 13.11.2023
Winter 2023/2024

Outline

- Habitable Zone
- Biomarkers
- Discussion

The definition of the Habitable Zone

- James F. Kasting - 1993

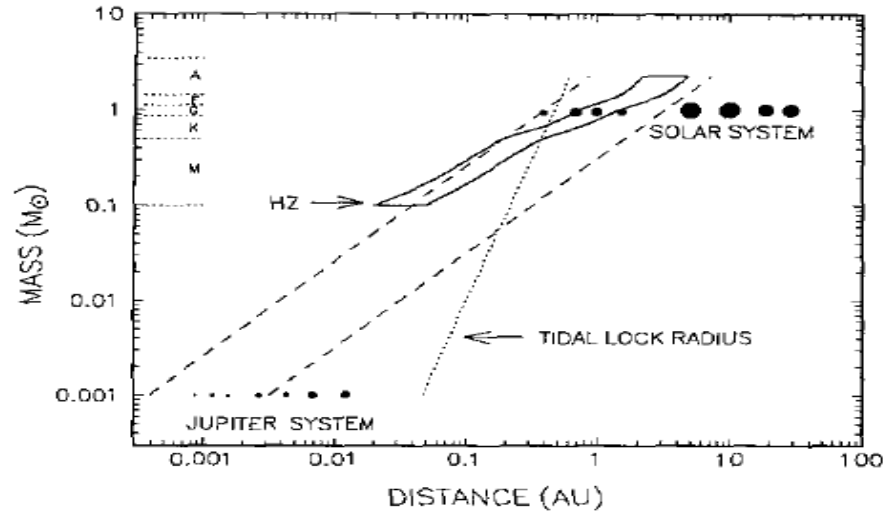
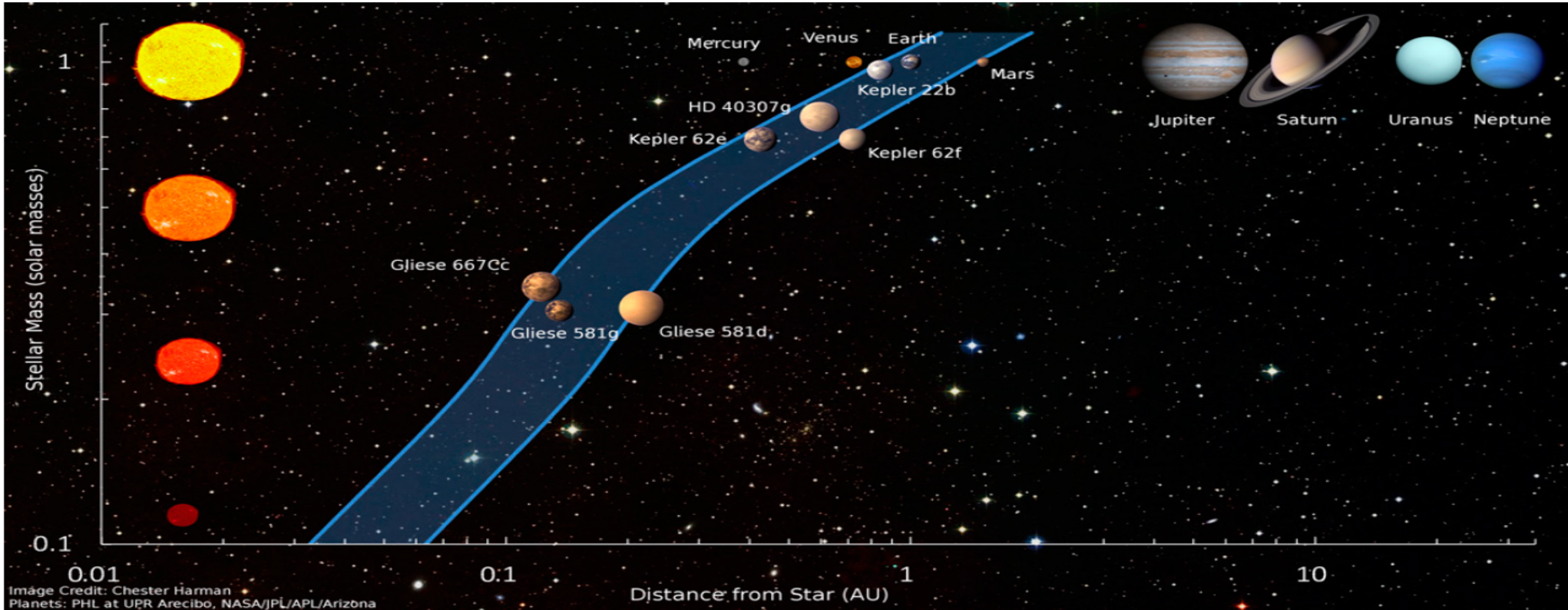


FIG. 16. Diagram showing the ZAMS habitable zone (solid curves) as a function of stellar mass (intermediate habitability estimates used). The long-dashed lines delineate the probable terrestrial planet accretion zone. The dotted line represents the distance at which an Earth-like planet in a circular orbit would be locked into synchronous rotation within 4.5 Gyr as a result of tidal damping. Note that all Earth-like planets within the HZ of an M star would be within this radius.

The habitable zone



Extending the HZ

- H₂ rich Super Earth atmospheres and planets with volcanic activity extend the HZ
- Ramirez et al. 2017,

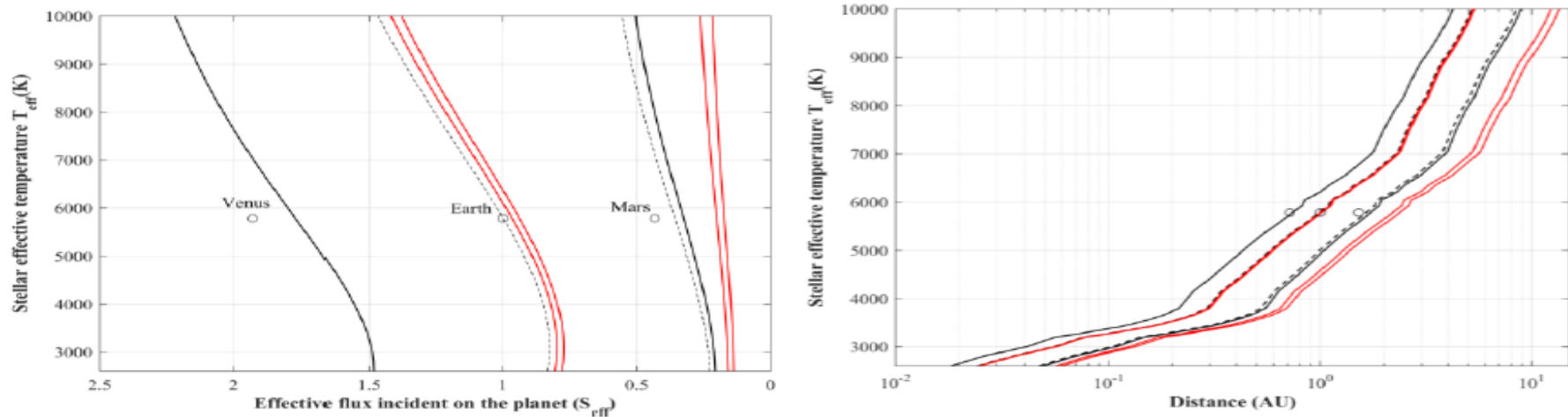


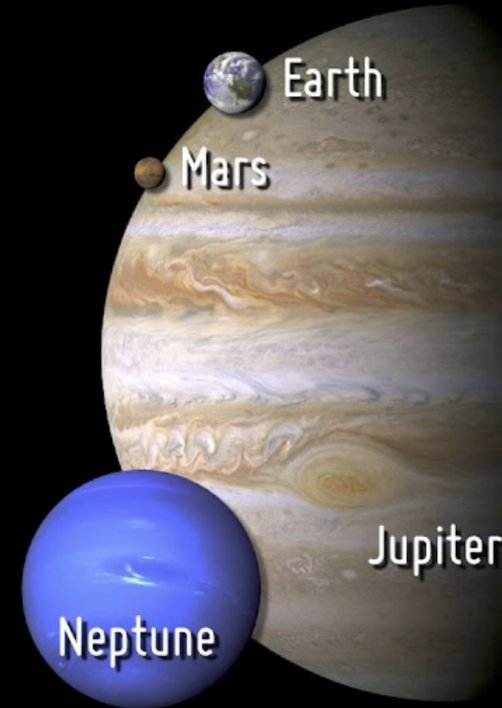
Figure 2: Effective stellar temperature versus (left) incident stellar flux (S_{eff}) and (right) orbital distance for the classical (dashed), empirical (solid black), and volcanic hydrogen (solid red) habitable zone. The red curves contain 30% and 50% H₂, respectively. As shown in Kopparapu et al. (2013), Earth appears near the classical inner edge because of the generic model assumption of 100% relative humidity. With subsaturation, Earth is well within the classical HZ (e.g., Leconte et al. 2013)

Sample of 2015/2016 (today 63)

Potentially Habitable Exoplanets



Sorted by Distance from Earth



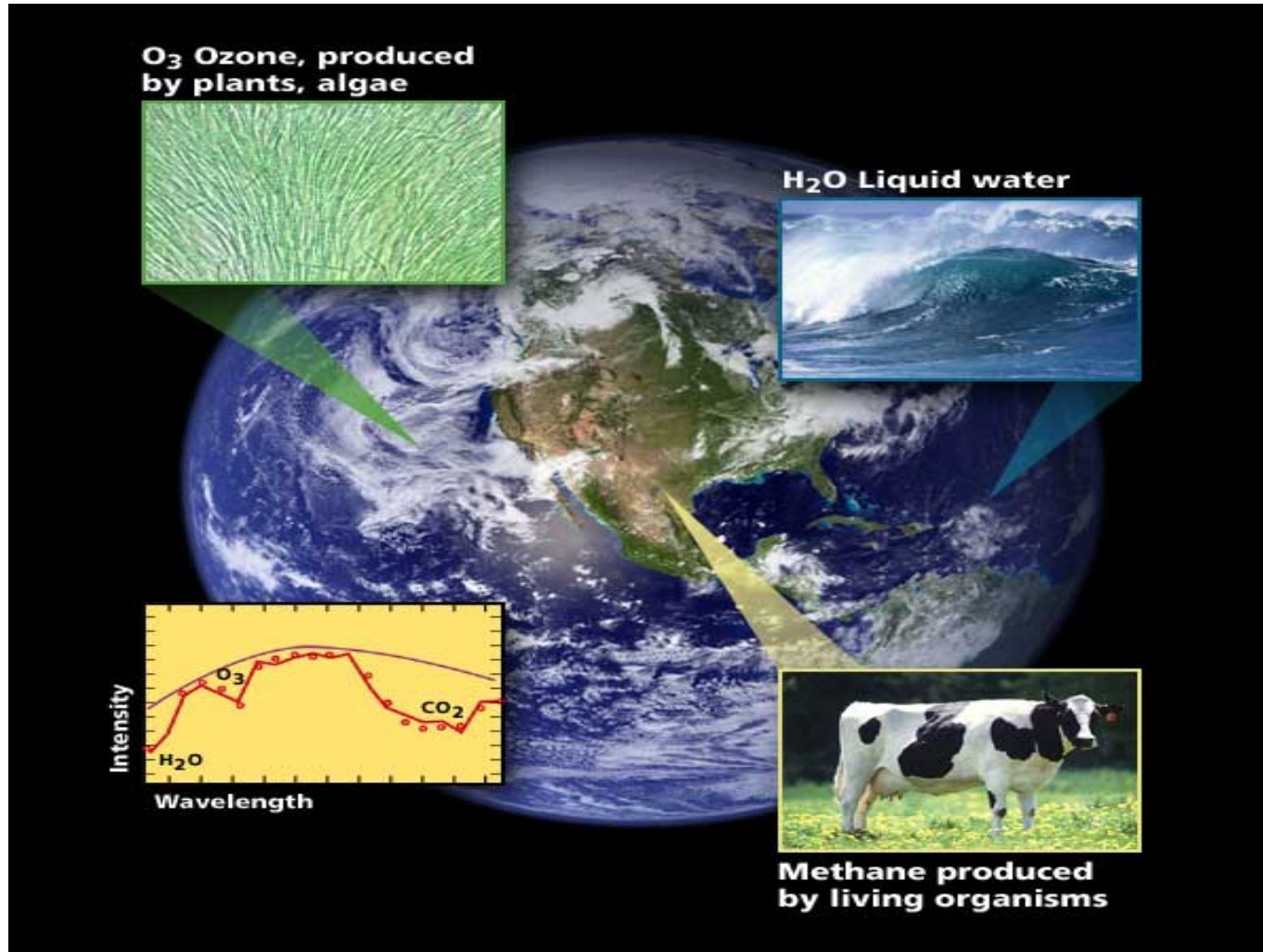
Artistic representations. Earth, Mars, Jupiter, and Neptune for scale. Distance from Earth in light years (ly) is between brackets.

CREDIT: PHL @ UPR Arcibo (phl.upr.edu) Jan 5, 2023

Habitable planets today

- <http://phl.upr.edu/projects/habitable-exoplanets-catalog>

Biosignature



Biosignature - papers

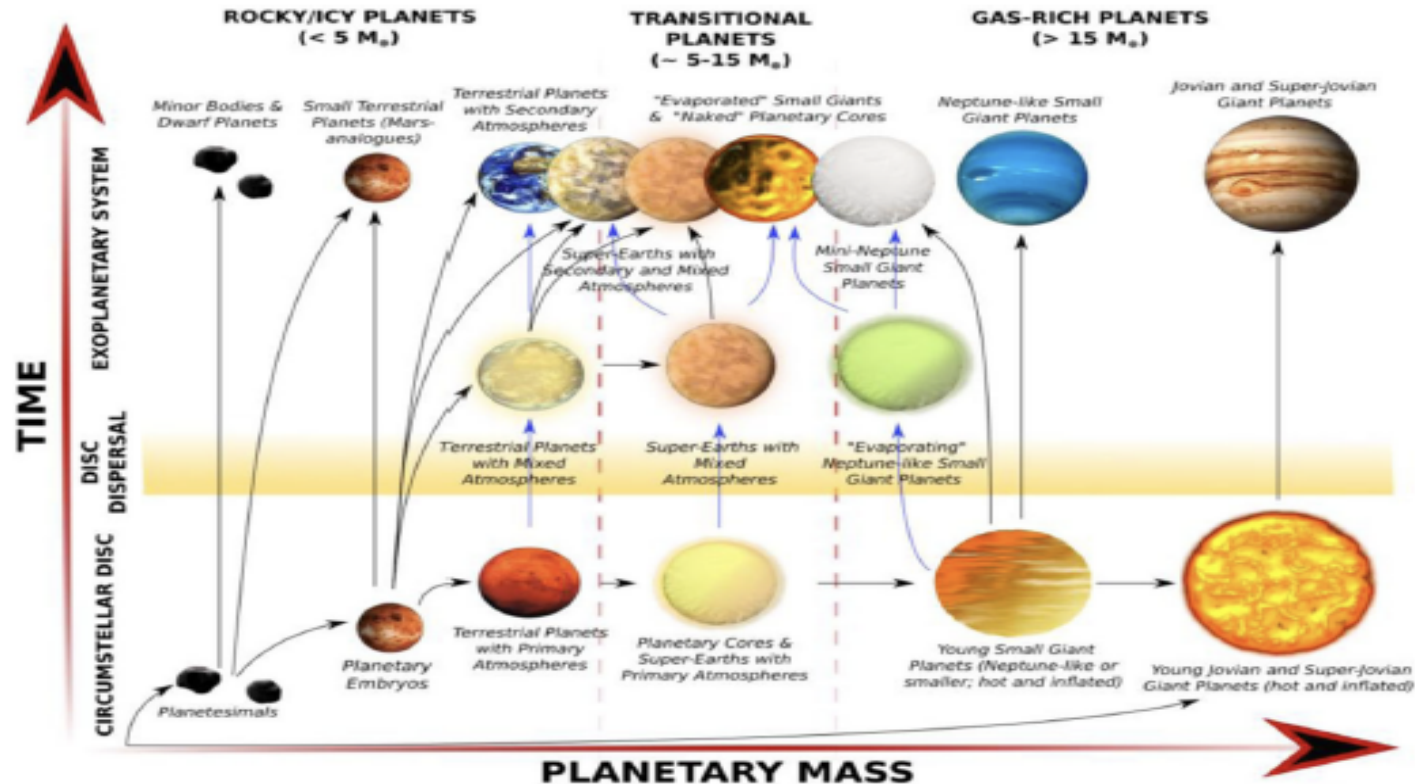
Seager and Bains -

<https://www.science.org/doi/10.1126/sciadv.1500047>

L. Kaltenegger et al. <https://arxiv.org/pdf/astro-ph/0609398.pdf>

Spectrum of the Earth

Atmosféry klíč k životu jak ho známe ze Země



TOI-700 example models

ATMOSPHERIC MODELING OF TOI-700 D

7

#	Archetype	Surface type	Surface pressure (bar)	Primary atmospheric constituent	Minor constituents, partial pressures (bar)	Rotation	Surface temperature (K)	TOA albedo	Sea ice fraction (%)	Stratospheric water vapor (kg/kg)
1	Plain	aqua	1	N ₂	H ₂ O	synchronous	236.7	0.3968	76.2%	6.5014e-8
2	Modern Earth	aqua	1	N ₂	H ₂ O CO ₂ (4e-4) CH ₄ (1.7e-6)	synchronous	246.7	0.3893	71.2%	3.605e-7
3	Modern Earth	land	1	N ₂	H ₂ O CO ₂ (4e-4) CH ₄ (1.7e-6)	synchronous	232.7	0.2840	N/A	N/A
4	Archean Earth	aqua	1	N ₂	H ₂ O CO ₂ (0.01) CH ₄ (1.0e-4)	synchronous	258.4	0.3594	66.3%	7.316e-7
5	Archean Earth	aqua	1	N ₂	H ₂ O CO ₂ (0.1) CH ₄ (1.0e-3)	synchronous	263.2	0.3988	62.3%	2.644e-5
6	Archean Earth	aqua	1	N ₂	H ₂ O CO ₂ (0.1) CH ₄ (2.0e-3)	synchronous	263.7	0.3998	61.6%	3.645e-5
7	Archean Earth	land	1	N ₂	H ₂ O CO ₂ (0.1) CH ₄ (1.0e-3)	synchronous	251.5	0.2455	N/A	N/A
8	Archean Earth	aqua	0.5	N ₂	H ₂ O CO ₂ (0.1) CH ₄ (1.0e-3)	synchronous	256.8	0.3906	67.3%	5.615e-5
9	Archean Earth	aqua	4	N ₂	H ₂ O CO ₂ (0.1) CH ₄ (1.0e-3)	synchronous	307.2	0.317	0	6.406e-6
10	Archean Earth	aqua	10	N ₂	H ₂ O CO ₂ (0.1) CH ₄ (1.0e-3)	synchronous	360.8	0.2452	0	2.203e-6
11	Archean Earth	aqua	1	N ₂	H ₂ O CO ₂ (0.1) CH ₄ (1.0e-3)	2:1 resonant	325.7	0.131	0	6.095e-6
12	Archean Earth	land	1	N ₂	H ₂ O CO ₂ (0.1) CH ₄ (1.0e-3)	2:1 resonant	257.0	0.2547	N/A	N/A
13	H ₂ -supporting	aqua	1	N ₂	H ₂ O CO ₂ (0.1) CH ₄ (1.0e-3) H ₂ (0.1)	synchronous	267.6	0.394	60.3%	2.669e-5
14	Early Mars	aqua	0.5	CO ₂	H ₂ O	synchronous	266.2	0.3572	62.6%	2.802e-5
15	Early Mars	aqua	1	CO ₂	H ₂ O	synchronous	284.4	0.3775	0.05%	2.520e-5
16	Early Mars	aqua	2	CO ₂	H ₂ O	synchronous	324.3	0.2771	0%	3.027e-5
17	Early Mars	aqua	4	CO ₂	H ₂ O	synchronous	364.2	0.2214	0%	2.857e-4
18	Early Mars	land	1	CO ₂	none	synchronous	258.9	0.2304	N/A	N/A
19	Early Mars	land	4	CO ₂	none	synchronous	302.3	0.2165	N/A	N/A
20	Early Mars	land	10	CO ₂	none	synchronous	353.5	0.2310	N/A	N/A

Table 3. Global mean climatological properties for each of our simulations. By definition, sea ice fraction and stratospheric water vapor or not applicable for desiccated land planet cases. The stratospheric water vapor is taken at the model top, 0.01 mbar. All quantities given are in units of the mean.

TOI-700 example models

ATMOSPHERIC MODELING OF TOI-700 D

11

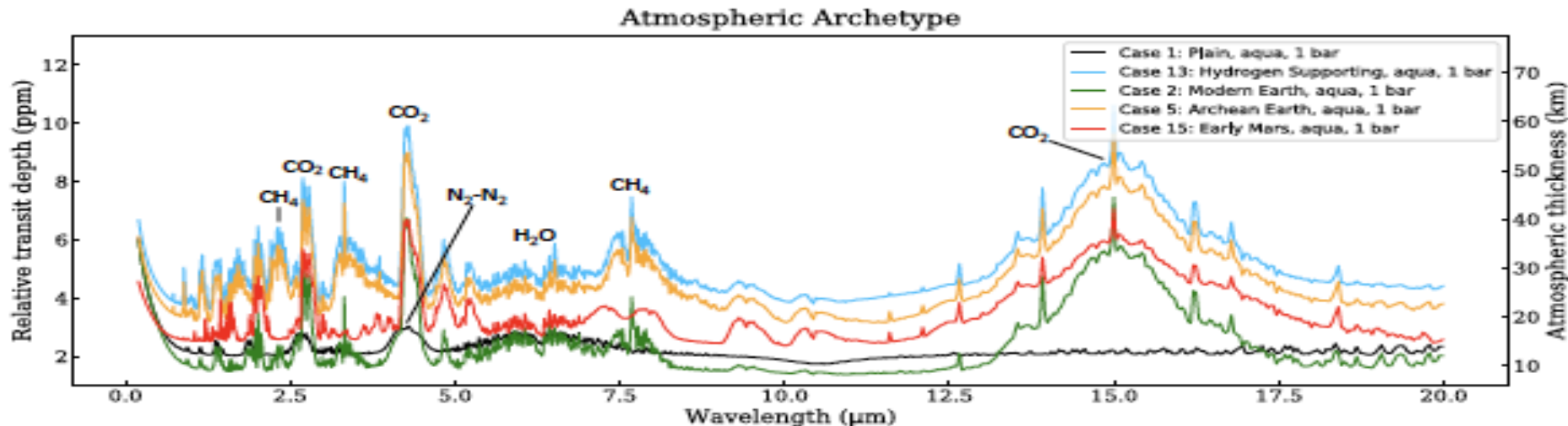


Figure 4. Comparison of transmission spectra for different atmospheric archetypes. All simulations shown here are ocean-covered and have a surface pressure of 1 bar. Prominent features are labeled. The spectrum for the “hydrogen-supporting” atmosphere (10% H_2) has both the highest continuum and the largest $15\mu\text{m}$ CO_2 feature.

TOI-700 example phase curves

18

SUISSA ET AL.

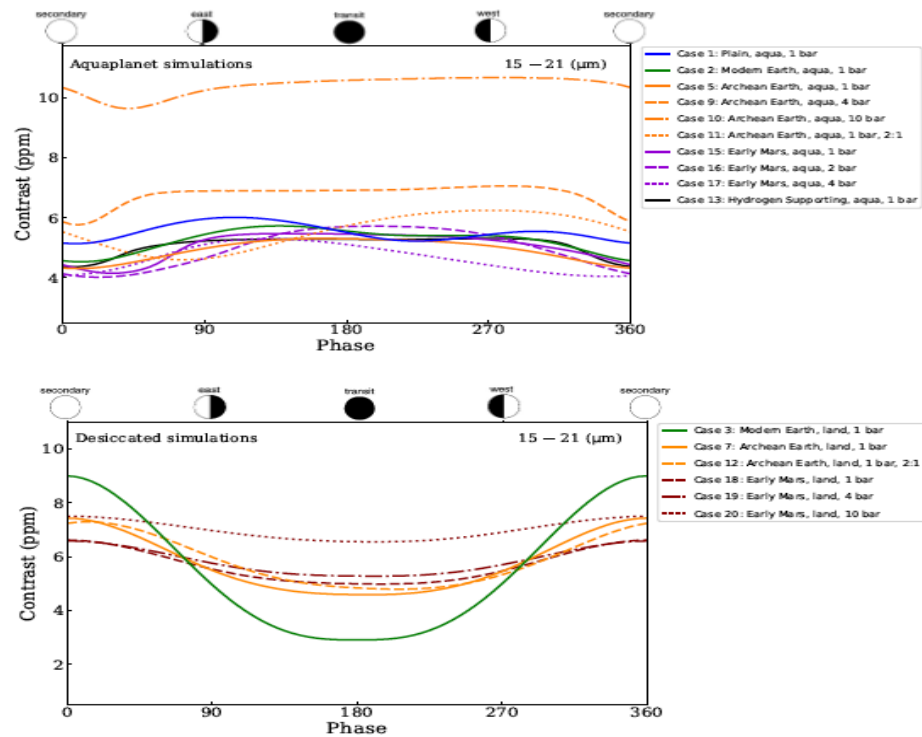
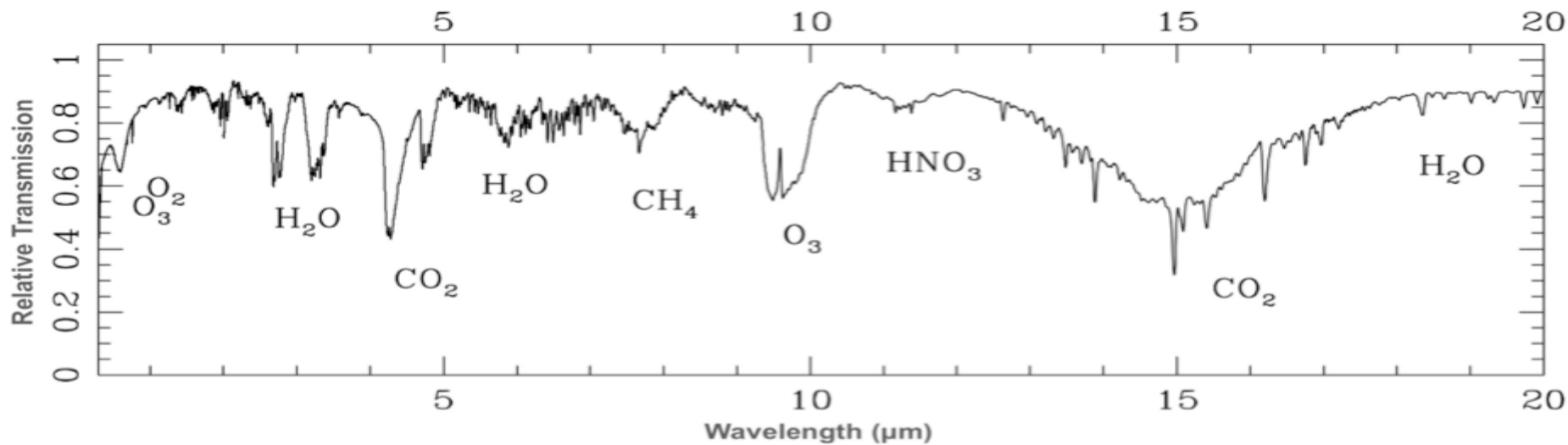
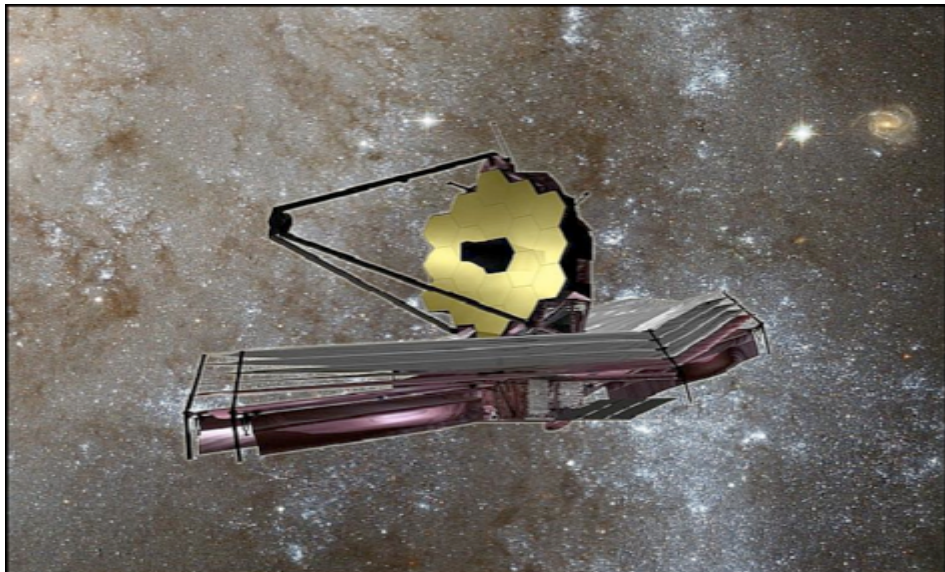


Figure 10. Phase curves for the majority of our simulations in this work. Aquaplanets are shown in the top panel; desiccated planets are shown in the bottom panel. Transit occurs at 180° . In the left panel, the contribution of reflected light dominates at wavelengths $< \sim 4.3 \mu\text{m}$, while thermally emitted light dominates at wavelengths $> \sim 4.3 \mu\text{m}$. In the right panel, the integrated fluxes for the phase curves are $15\text{--}21 \mu\text{m}$.



Kaltenegger, L. and Traub, W. (2009) Transits of Earth-Like Planets. *Astrophysical Journal*



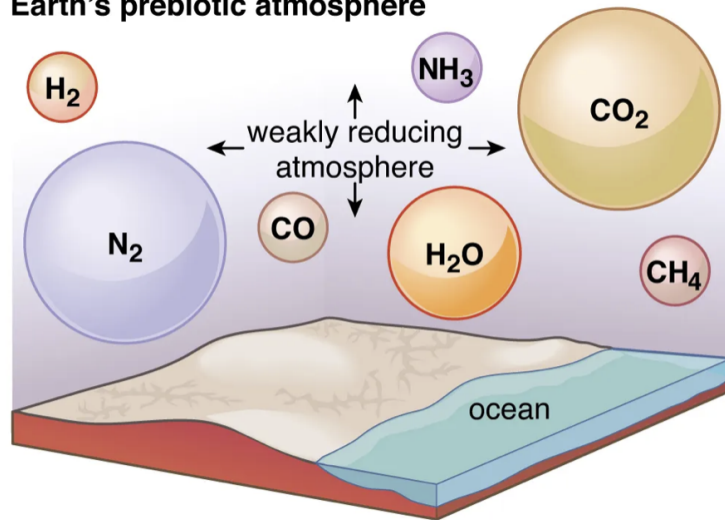
JWST

Launched!

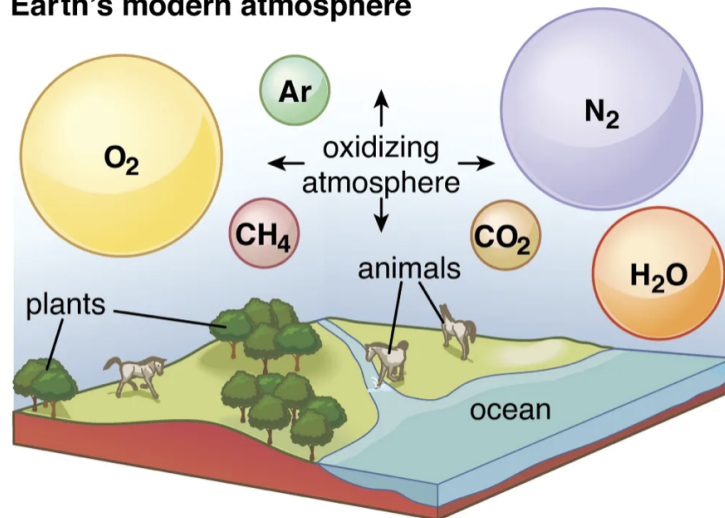
Ideal for characterization of small planets in infrared

Image NASA

Earth's prebiotic atmosphere



Earth's modern atmosphere



Albedo

- Albedo is the fraction of reflected light by the surface

- full reflection – $A=1$

Bond albedo

Geometric albedo

Albedo

- Albedo is the fraction of reflected light by the surface

- full reflection – $A=1$

Bond albedo

Geometric albedo

Albedo

- Albedo is the fraction of reflected light by the surface

- full reflection – $A=1$

Bond albedo

Geometric albedo

Albedo

- Albedo is the fraction of reflected light by the surface

- full reflection – $A=1$

Bond albedo

Geometric albedo

Albedo

- Albedo is the fraction of reflected light by the surface

- full reflection – $A=1$

Bond albedo

Geometric albedo

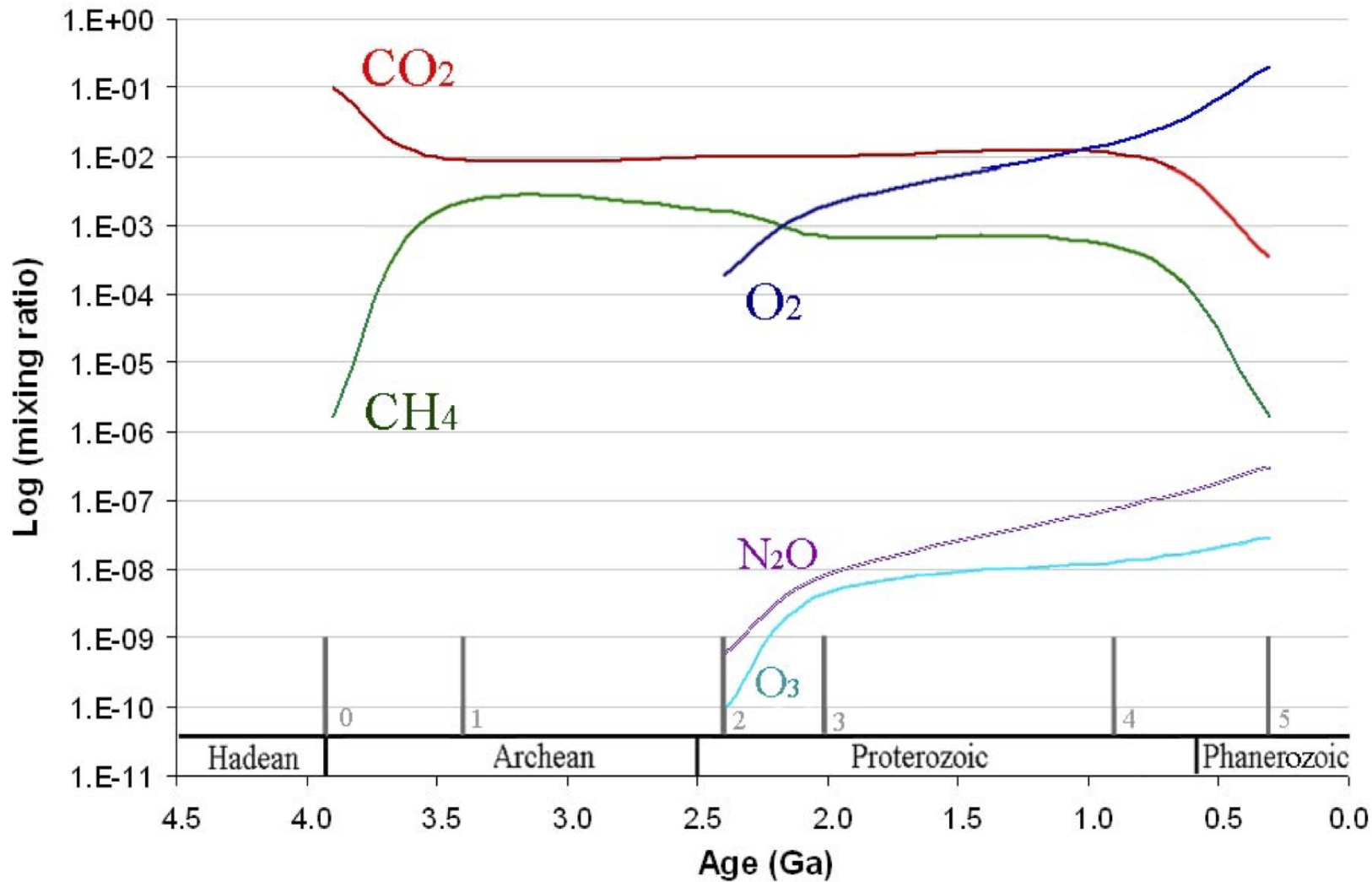
Albedo

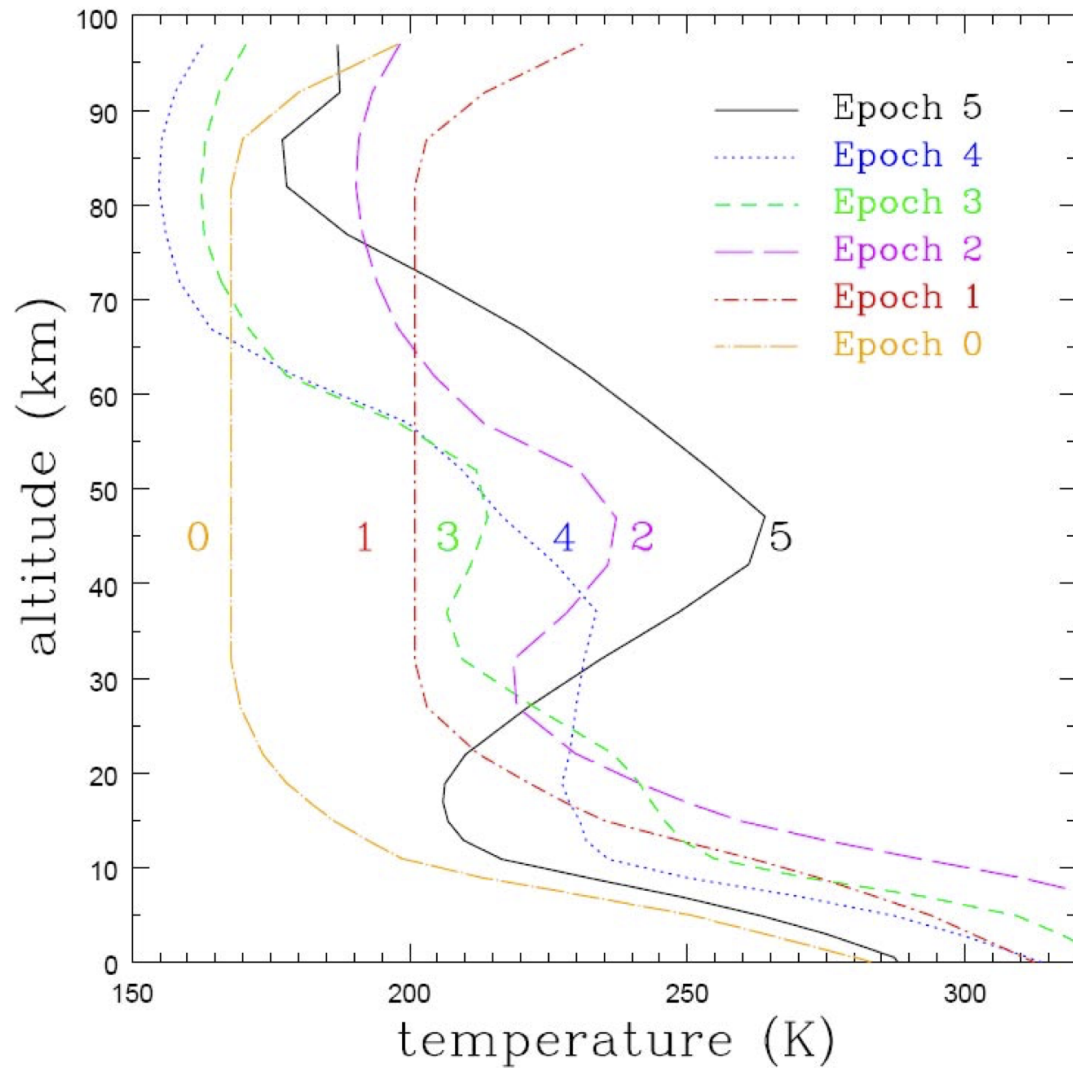
- Albedo is the fraction of reflected light by the surface

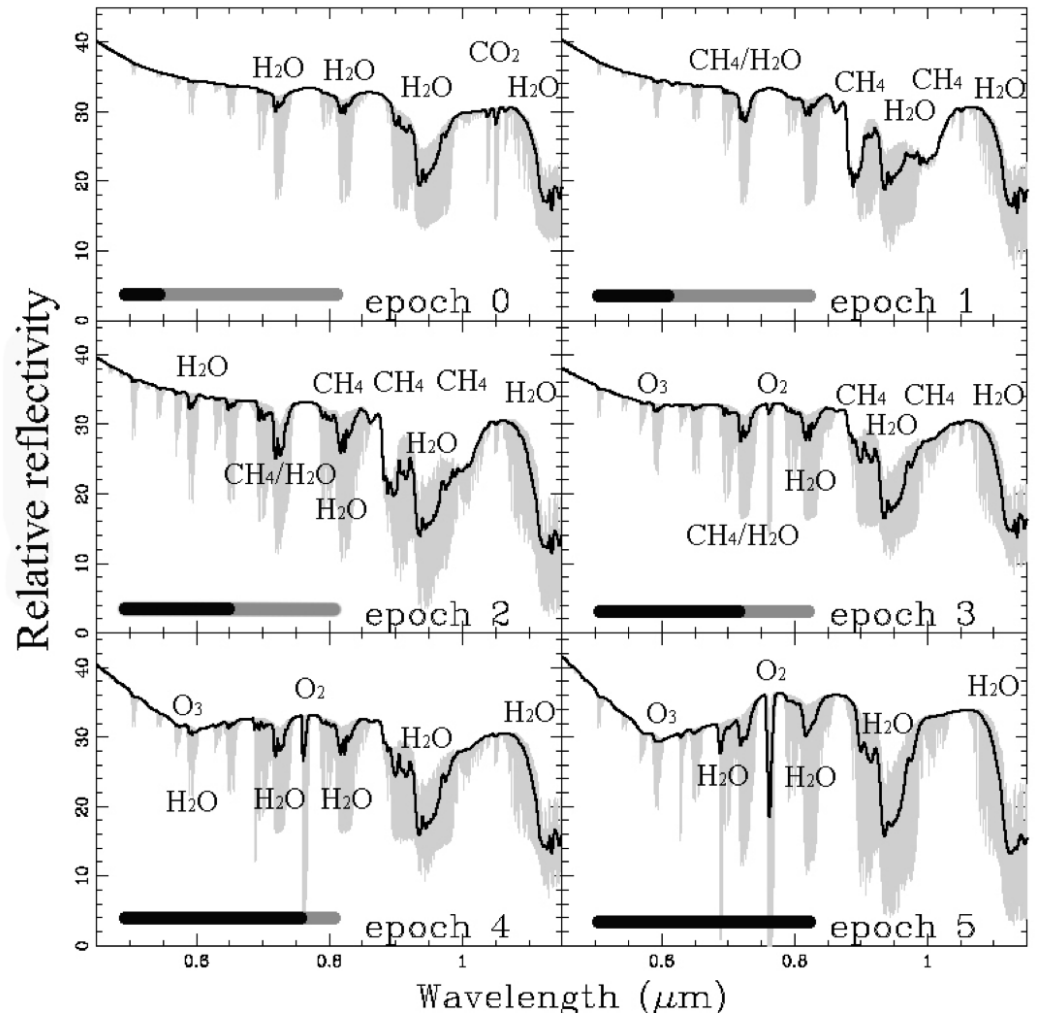
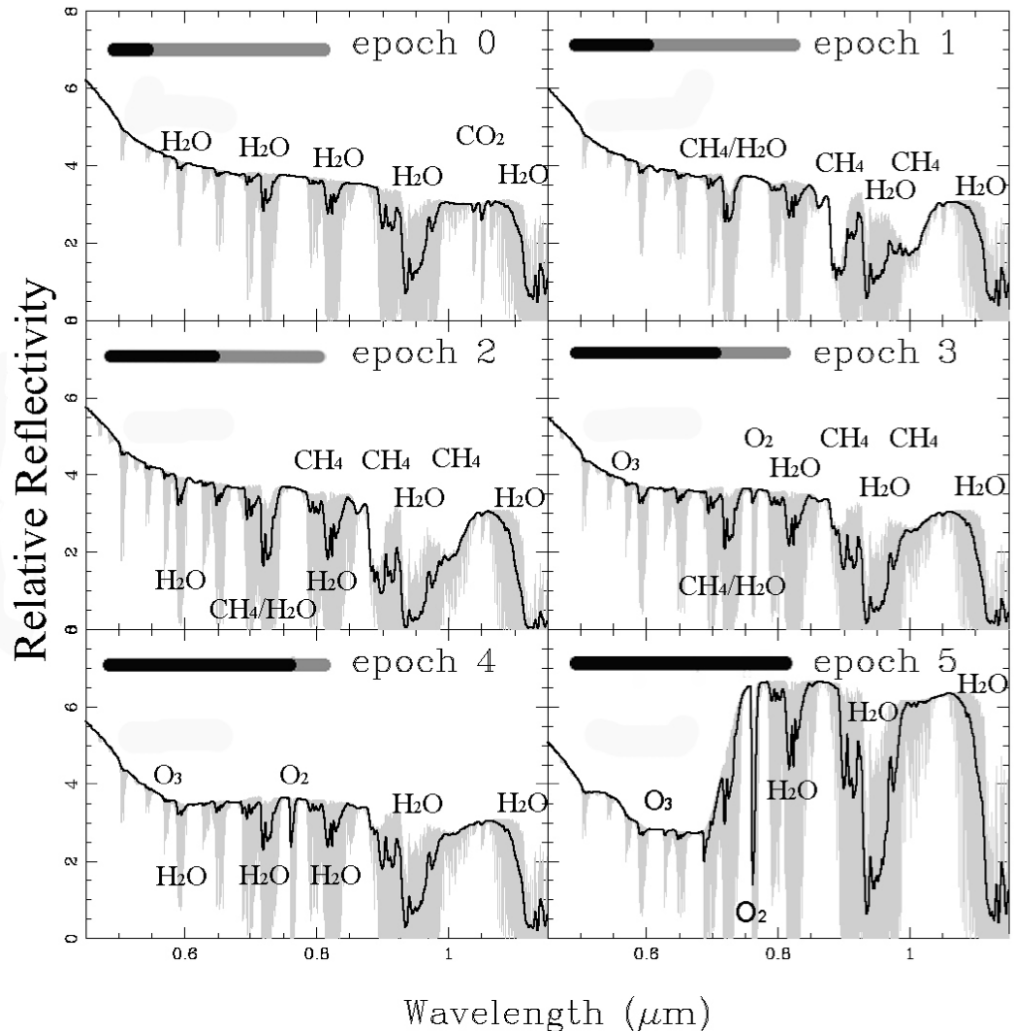
- full reflection – $A=1$

Bond albedo

Geometric albedo







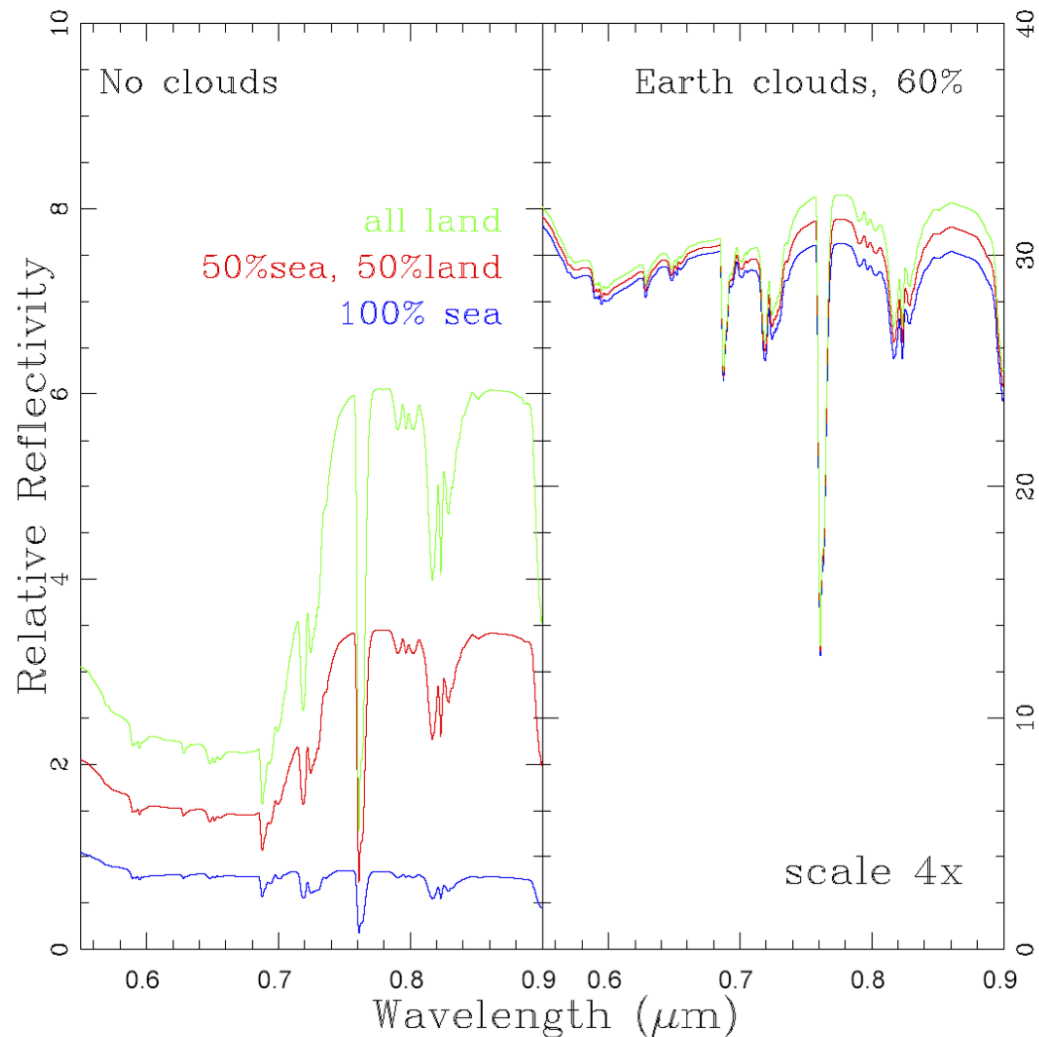
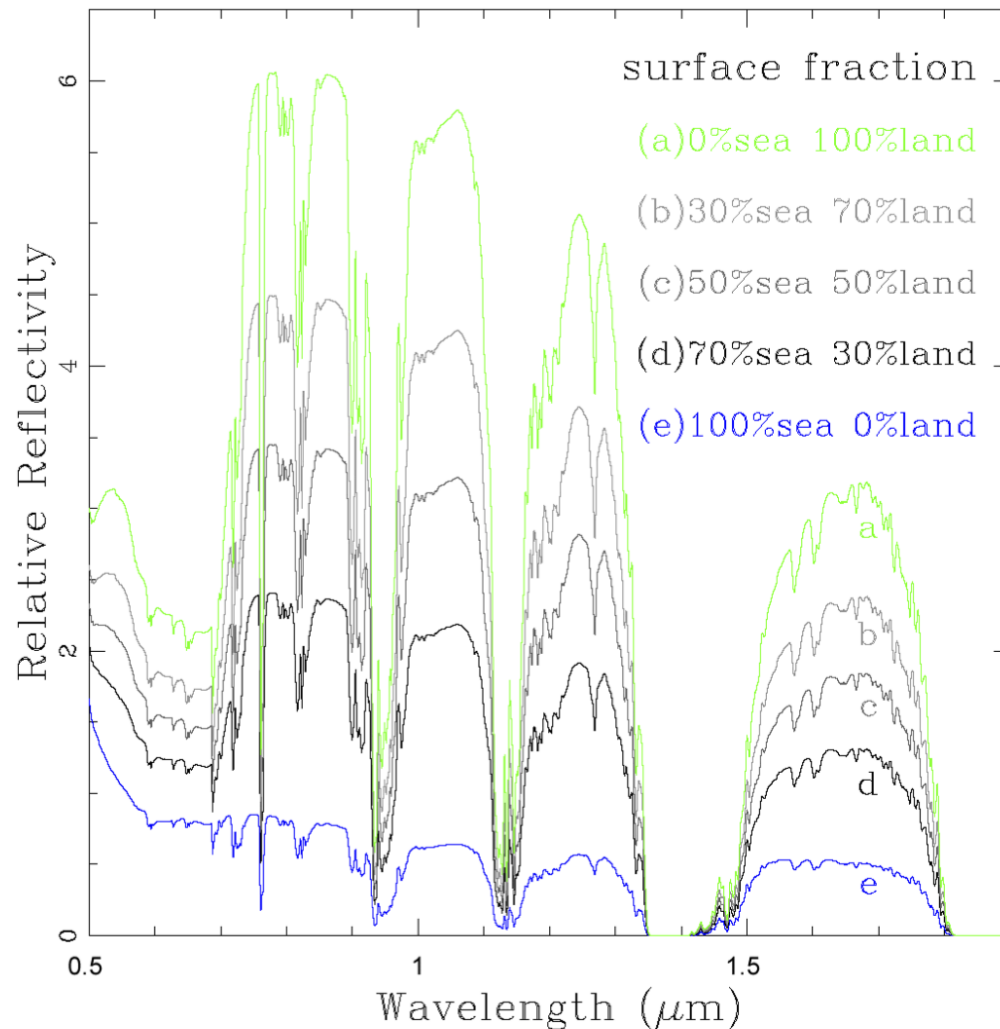
Albedo

- Albedo is the fraction of reflected light by the surface

- full reflection – $A=1$

Bond albedo

Geometric albedo



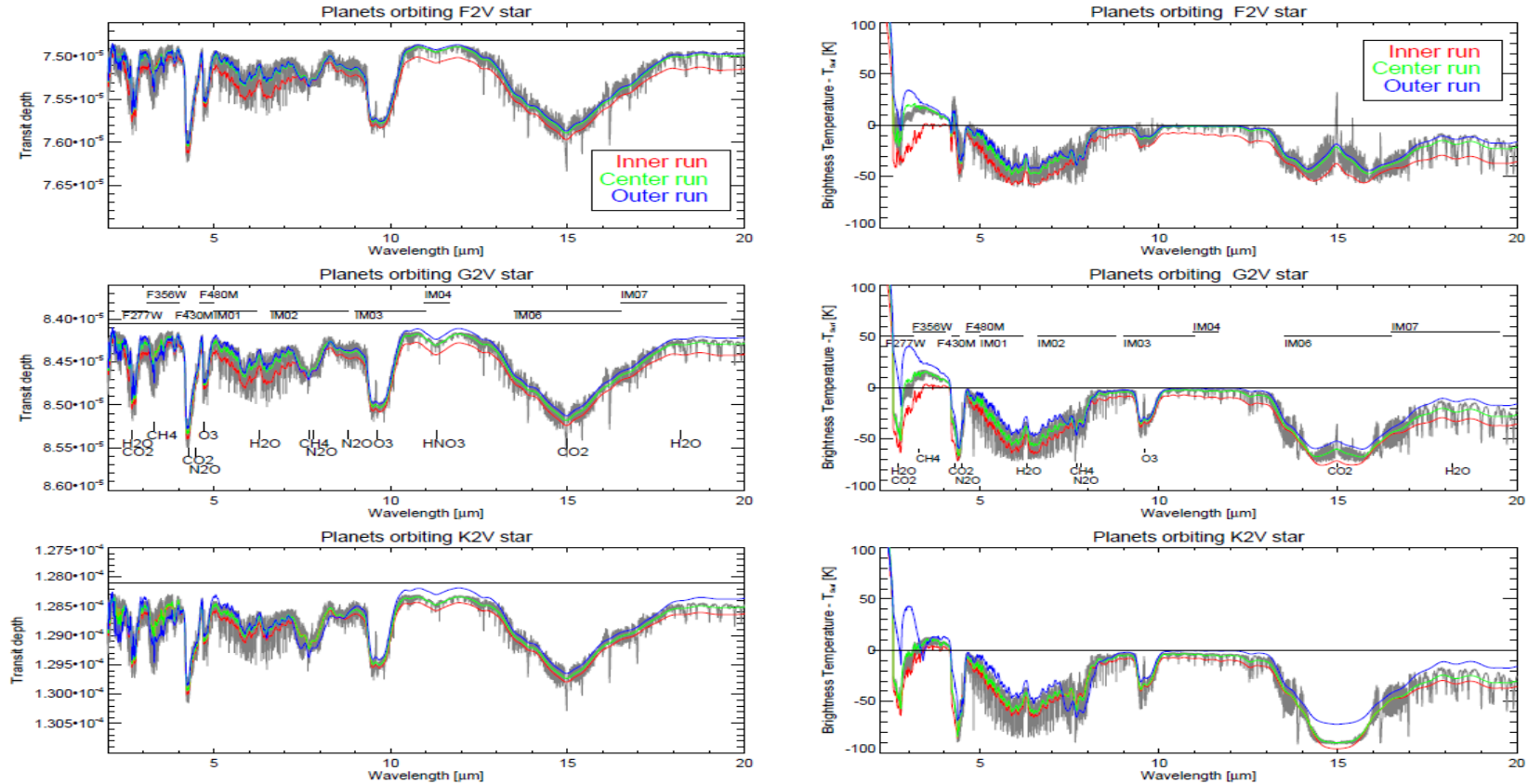
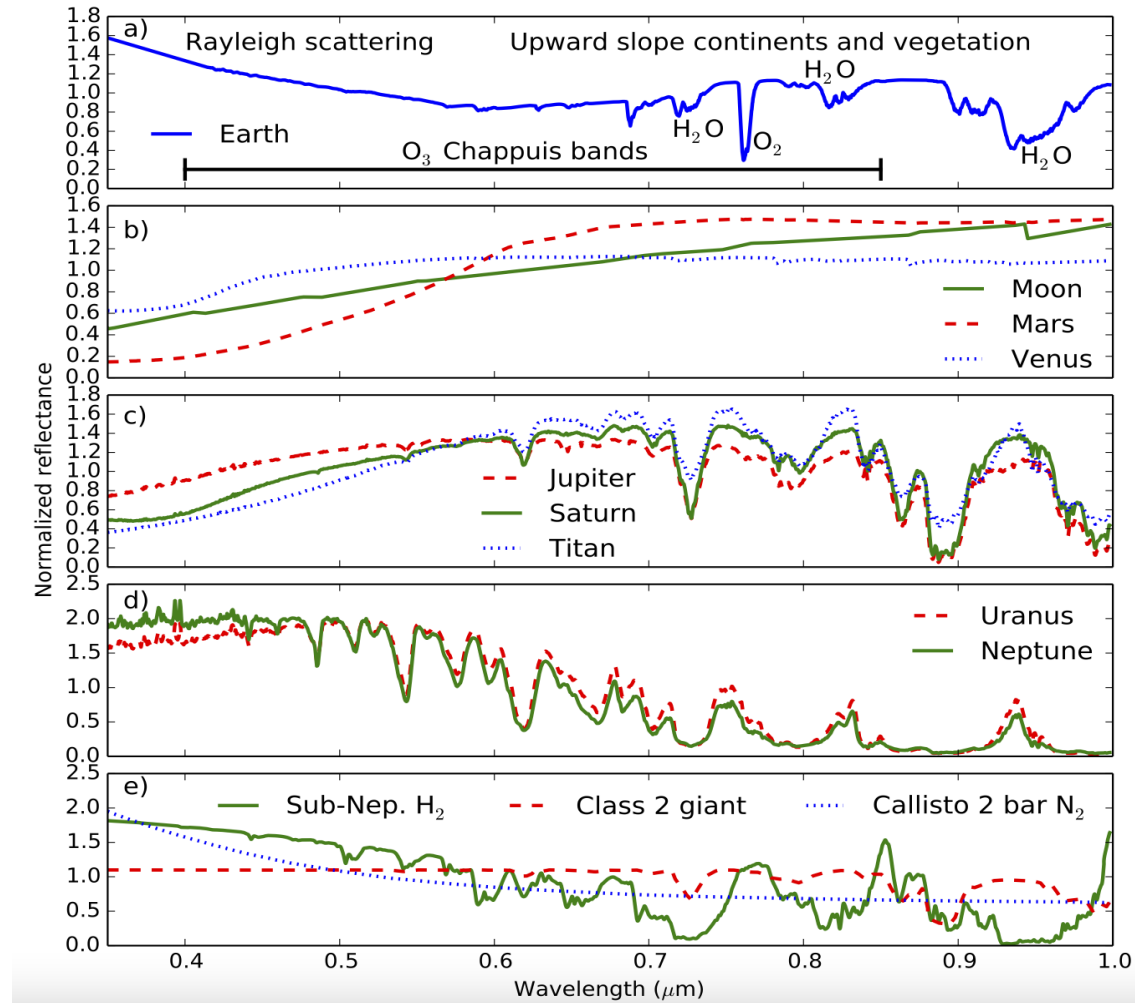
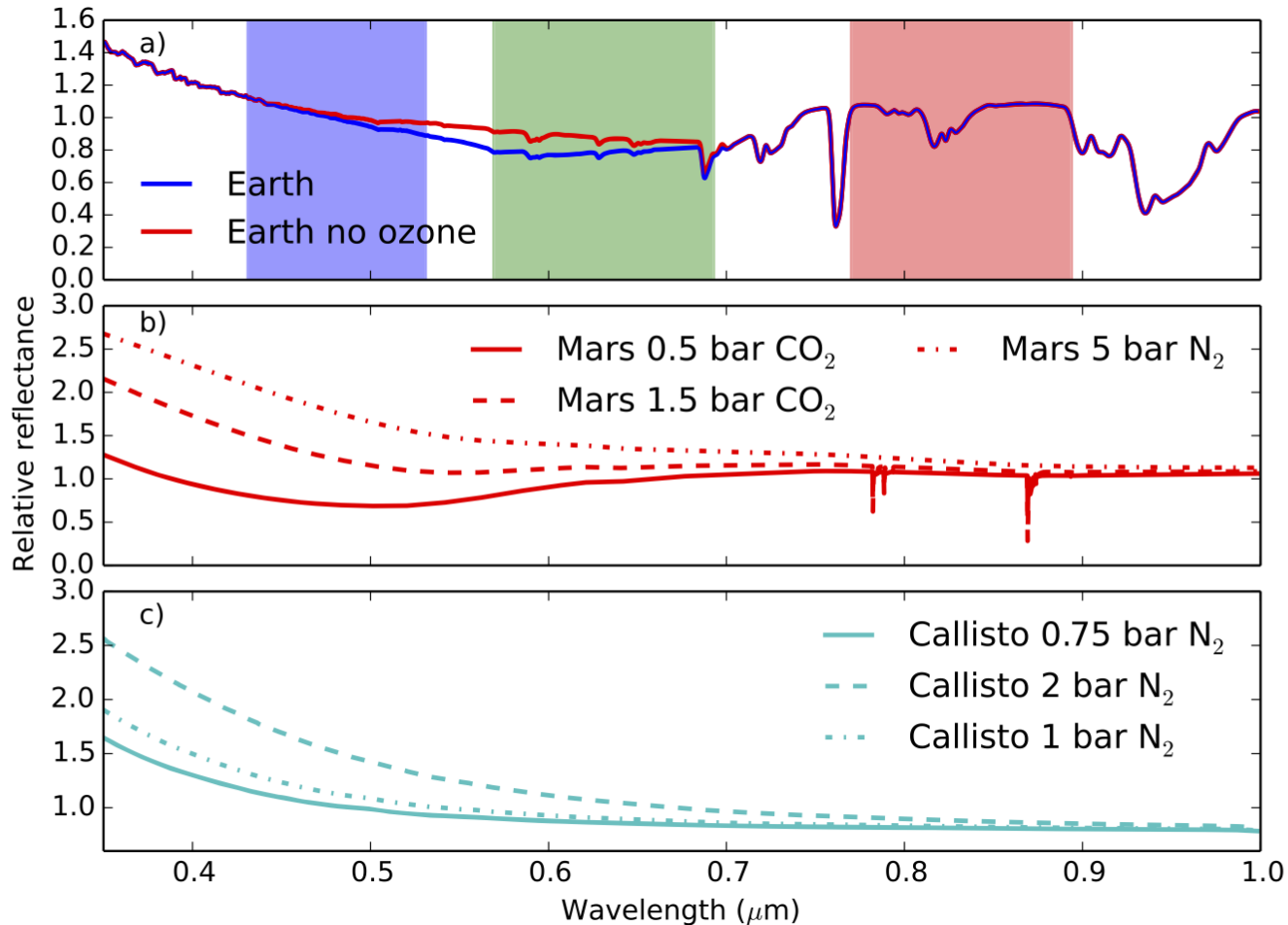


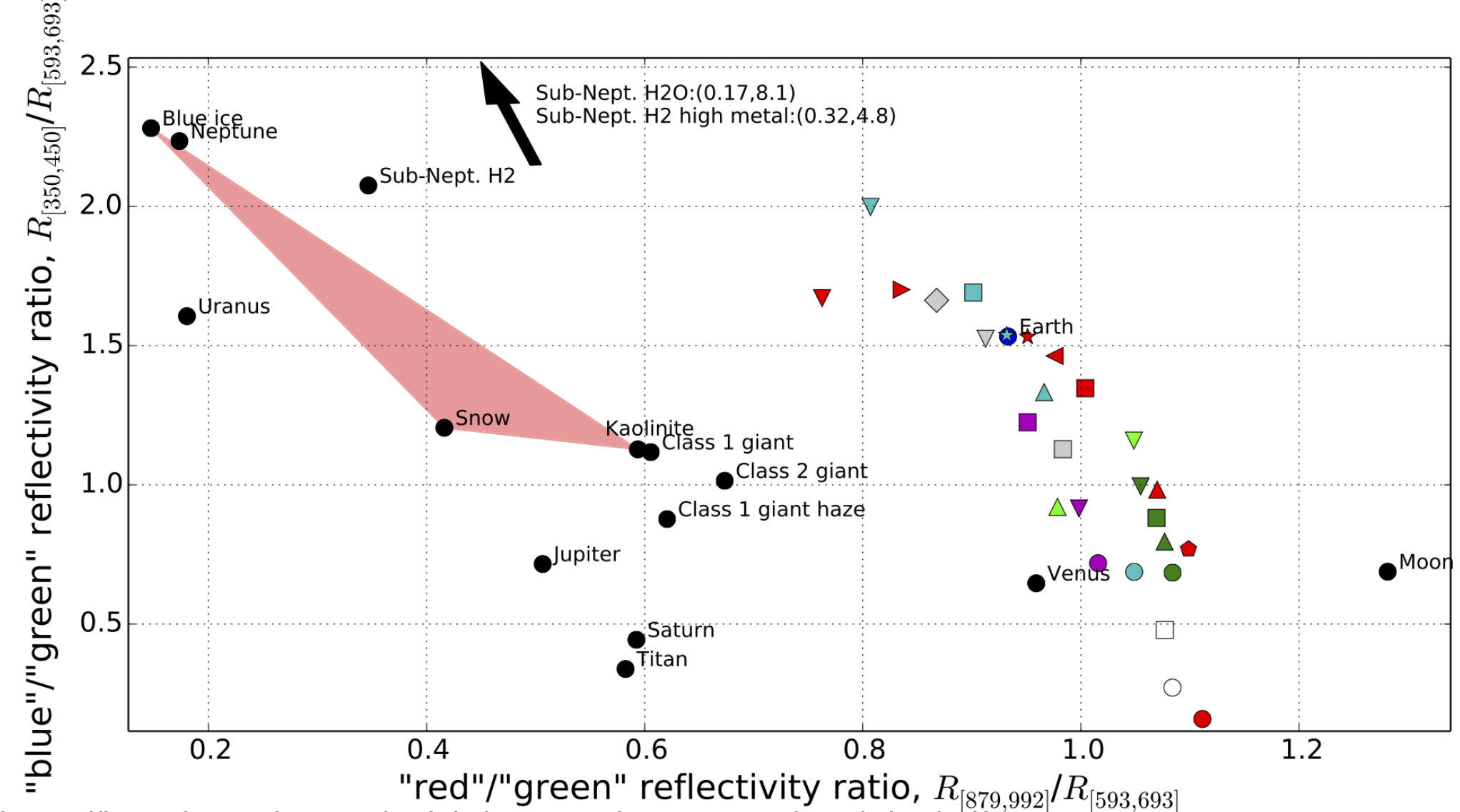
Fig. 4. Transit depth during primary eclipse (left) and brightness temperature difference with respect to the calculated surface temperature spectrum during secondary eclipse (right) for the scenarios considered. The spectral resolution is $R = 100$. Each center run with $R = 3000$ is shown in grey. The geometric transit depth (see Sect. 3.3) is indicated by a horizontal line for transmission spectra. The brightness temperature spectra include the reflected stellar component in the near-IR. Furthermore the bandpass of the filters considered in this work are shown.

How would different planets look like?



U shape – typical for the Earth






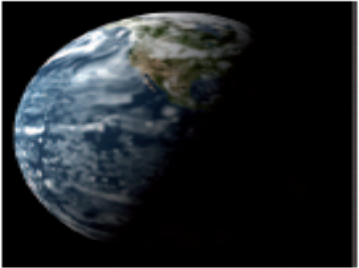
The Earthshine

- Sterzik et al. 2012, Nature

- Observing of the Earthshine reflected by the Moon

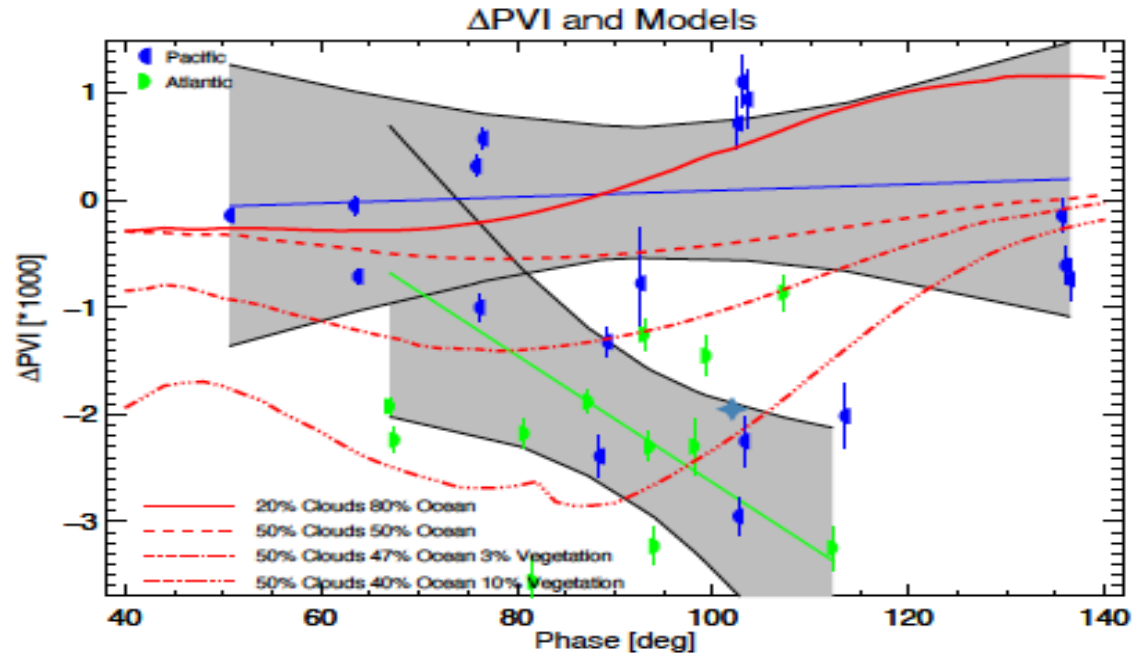
- FORS at VLT

- Polarization can help to describe the surface features

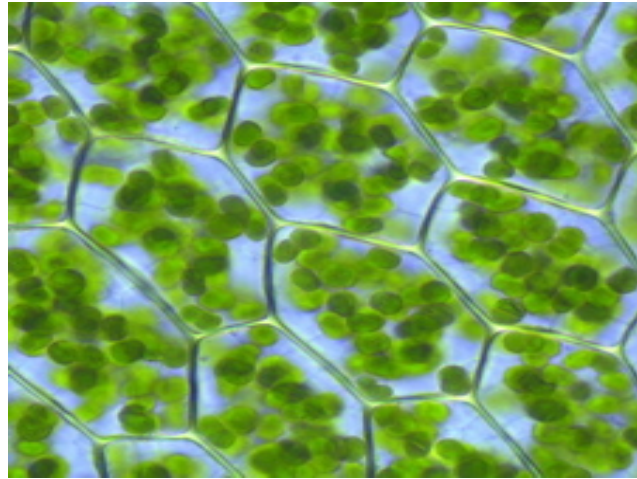
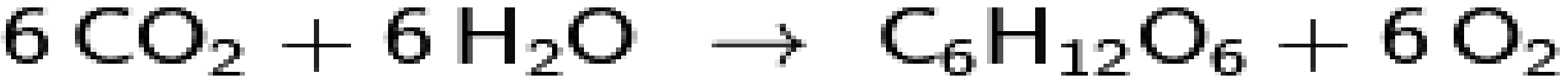
Observations	Observing date	
	25 April 2011, 09:00 ut	10 June 2011, 01:00 ut
View of Earth as seen from the Moon		
Sun–Earth–Moon phase (degrees)	87	102
Ocean fraction in Earthshine (%)	18	46
Vegetation fraction in Earthshine (%)	7	3
Tundra, shrub, ice and desert fraction in Earthshine (%)	3	1
Total cloud fraction in Earthshine (%)	72	50
Cloud fraction $\tau > 6$ (%)	42	27

The Earthshine

- The Atlantic side hints at decreasing PVI
- The Pacific side shows no correlation with PVI
- PVI is a Polarization Vegetation Index
- PVI reflects the difference of polarization between vegetated and not vegetated surfaces

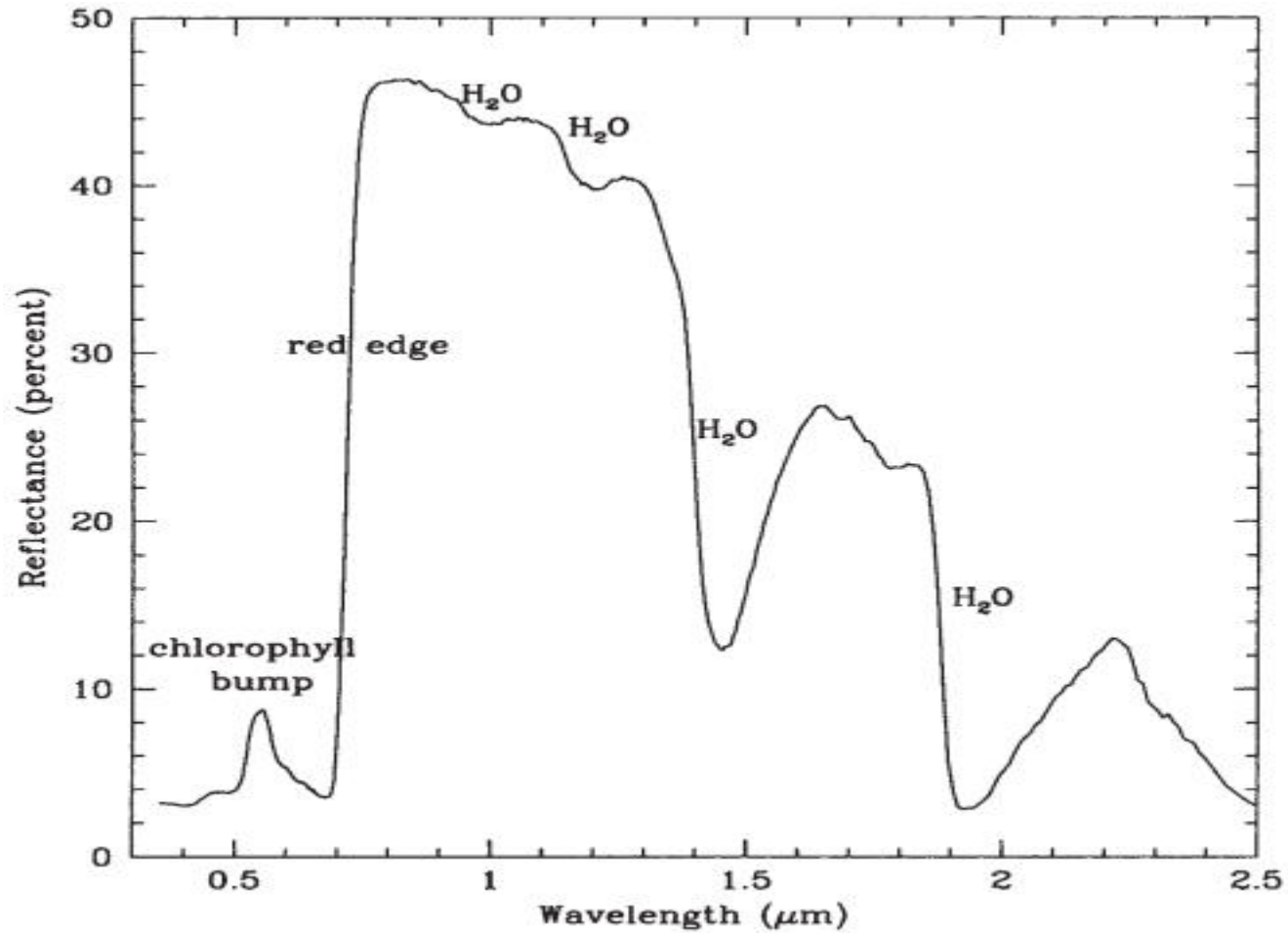


Photosynthesis



Chlorophyll - Credit: Wikimedia Commons

Red edge



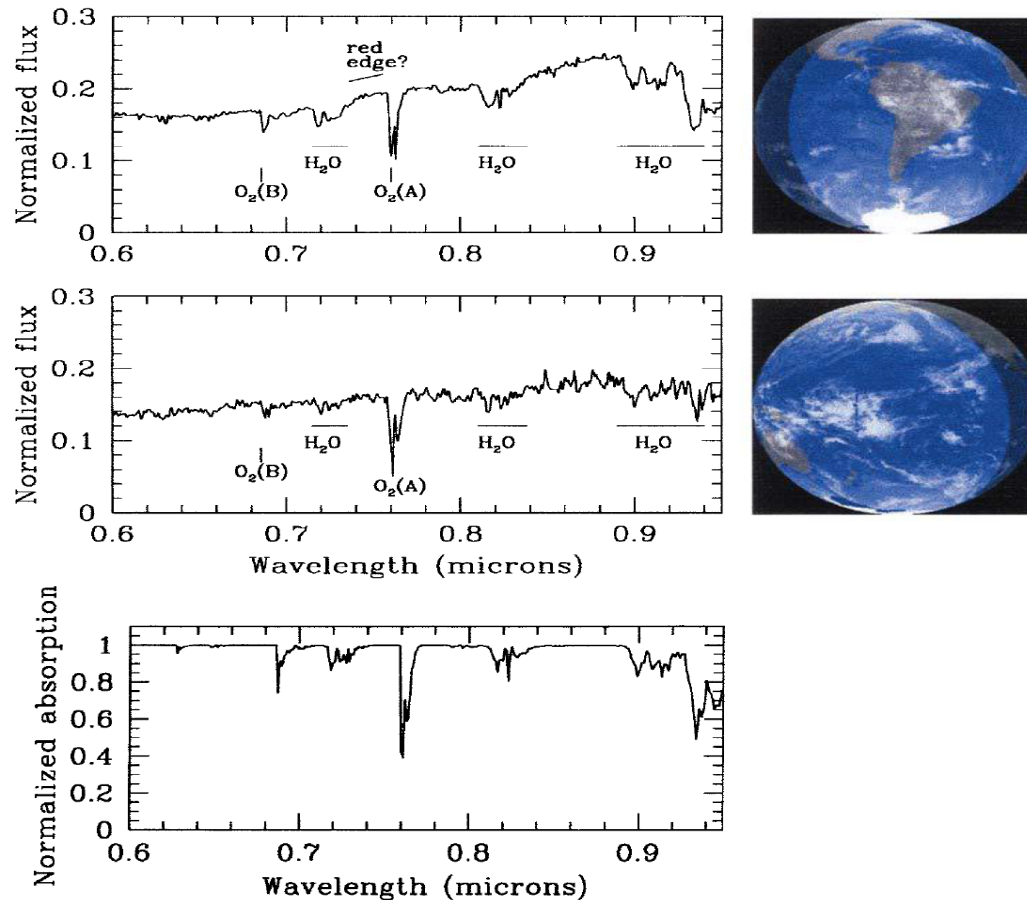
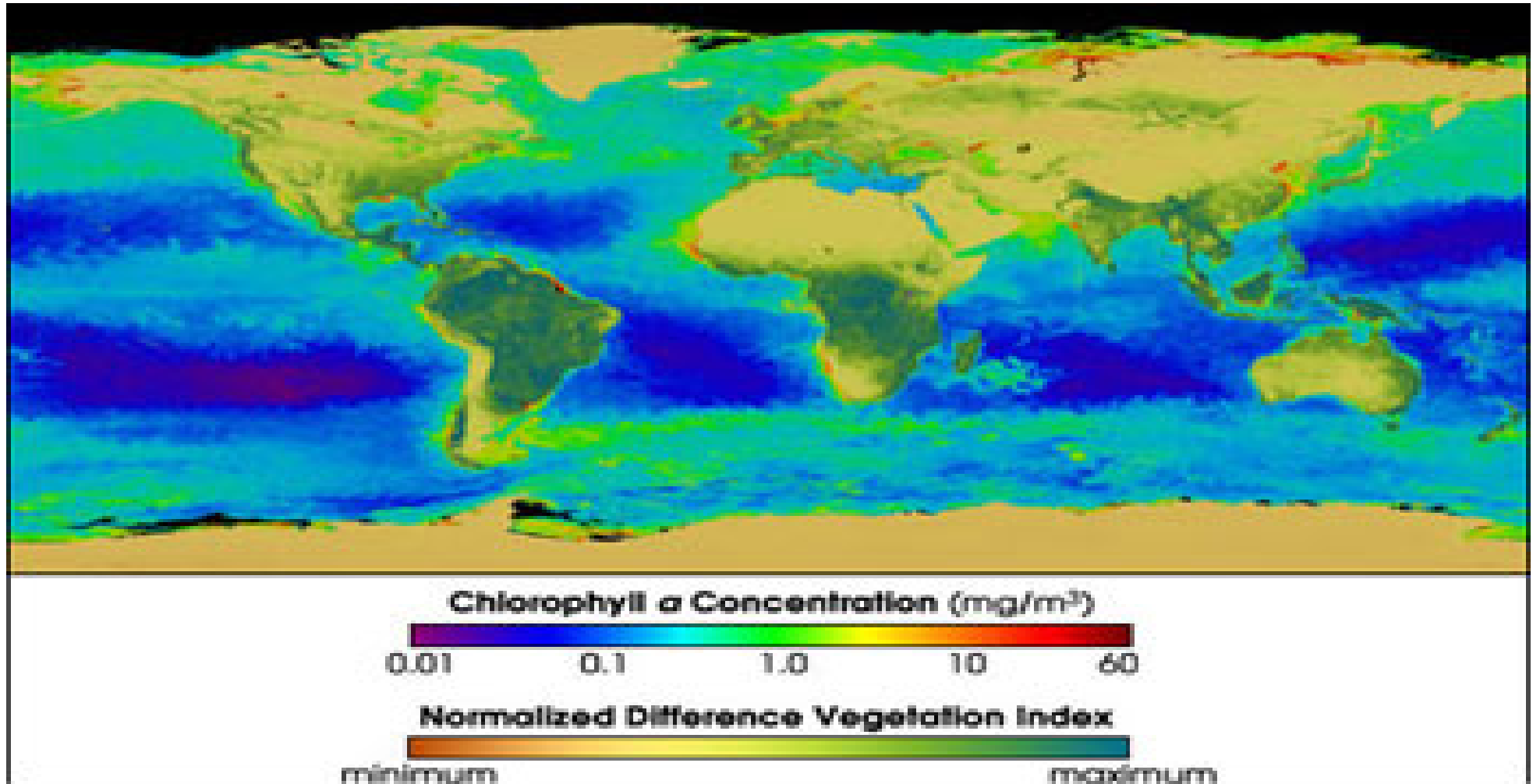
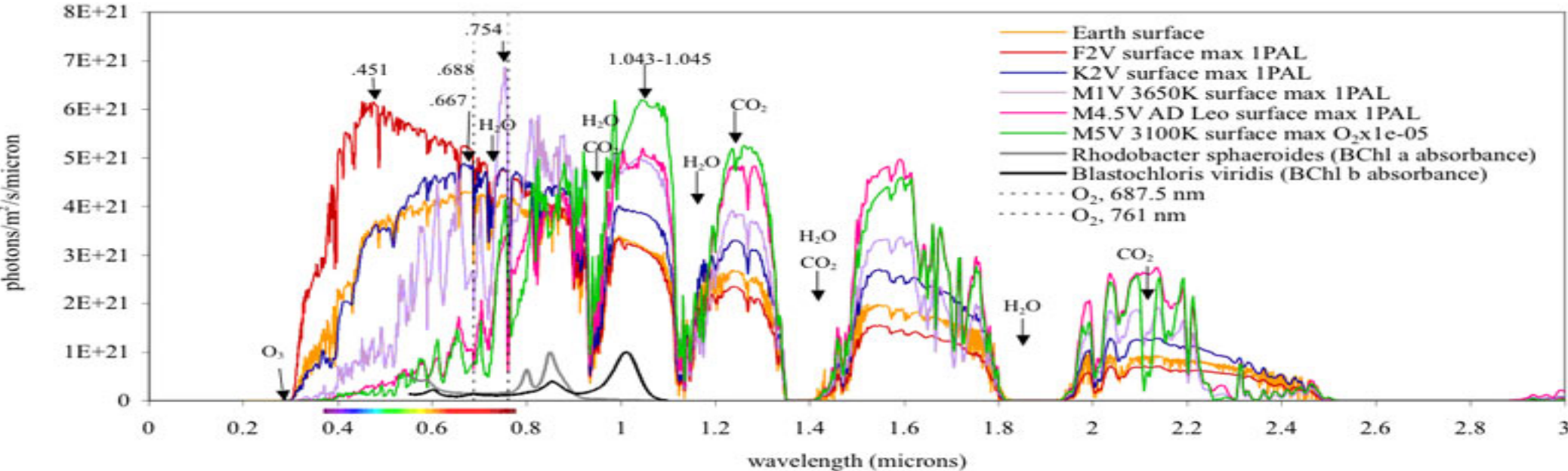


FIG. 4. Earthshine observations from APO. **Top panel:** Earthshine observations on 8 February 2002. The viewing geometry (including cloud coverage at the time of observations) of Earth from the Moon is shown in the right image (<http://www.fourmilab.ch/earthview/vplanet.html>). **Middle panel:** Same as the top panel for 16 February 2002. The viewing geometry of Earth includes much more vegetation in the top panel than in the middle panel. **Bottom panel:** An absorption spectrum through Earth's atmosphere from Kitt Peak National Observatory (<ftp://ftp.noao.edu/catalogs/atmospheric/transmission/>) smoothed to approximately the same resolution as the APO Earthshine data. Note the different y -axis on the absorption spectrum; the spectral features are much deeper than in the Earthshine spectrum, and there is no red edge feature.

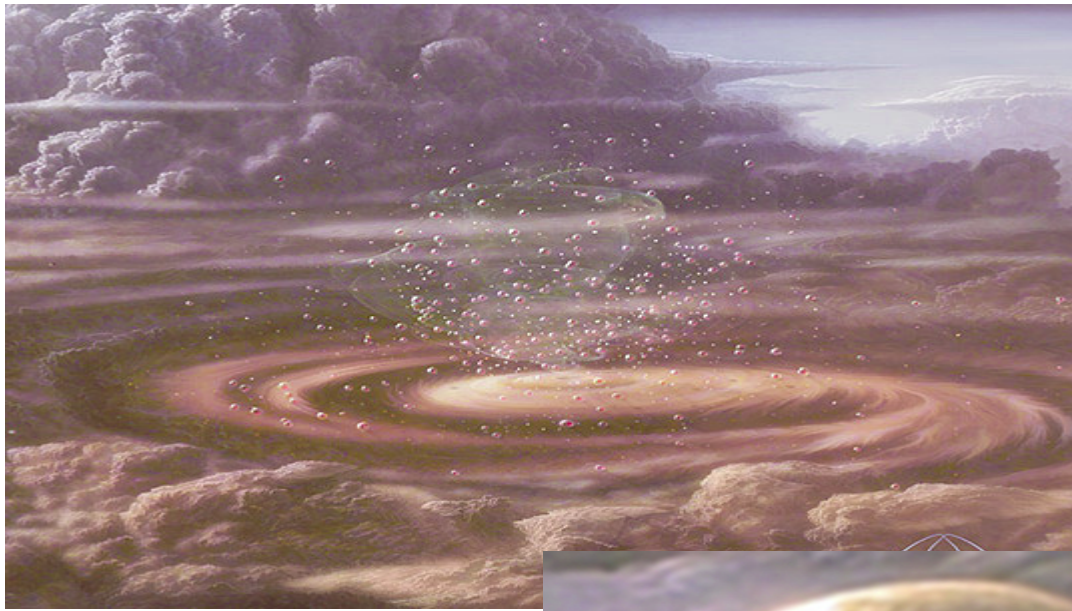


Credit: <http://www.giss.nasa.gov/research/news/20070411/>

How would be your vision?



Credit: <http://www.giss.nasa.gov/research/news/20070411/>



Credit: Carl Sagan Cosmos

Pyramids and others

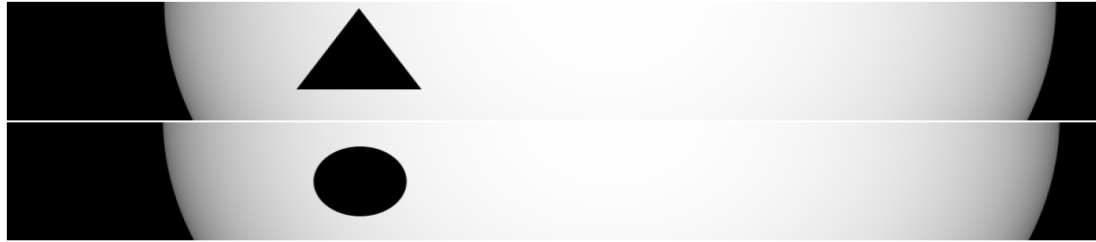
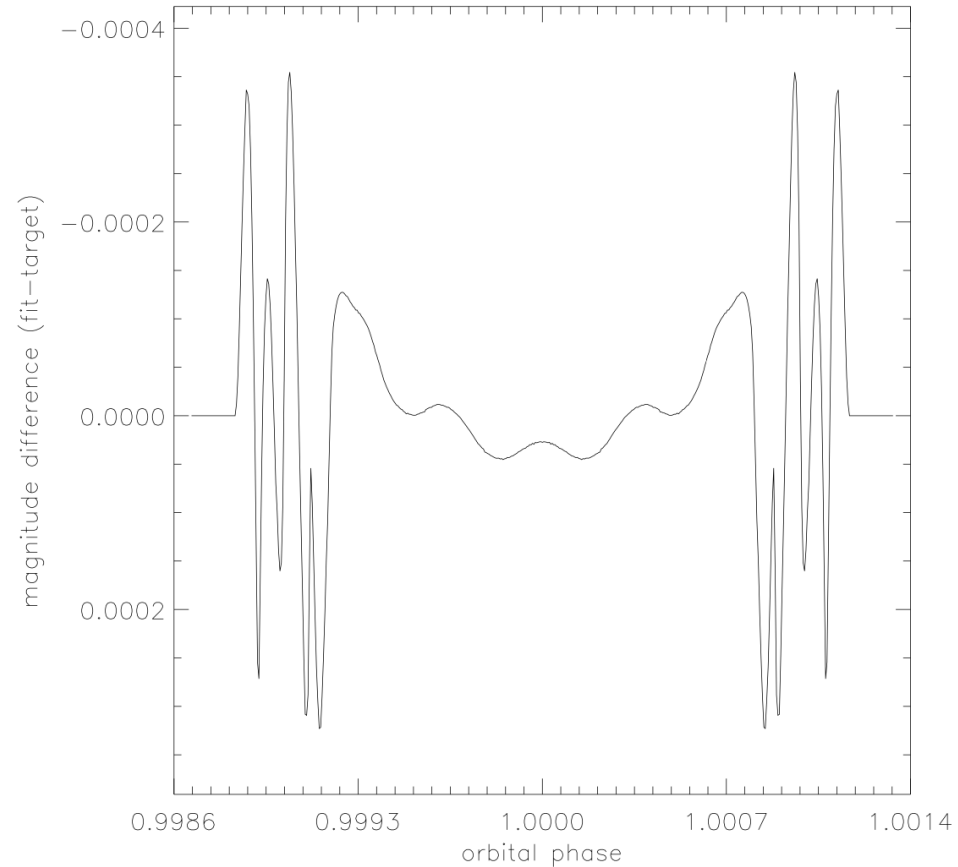
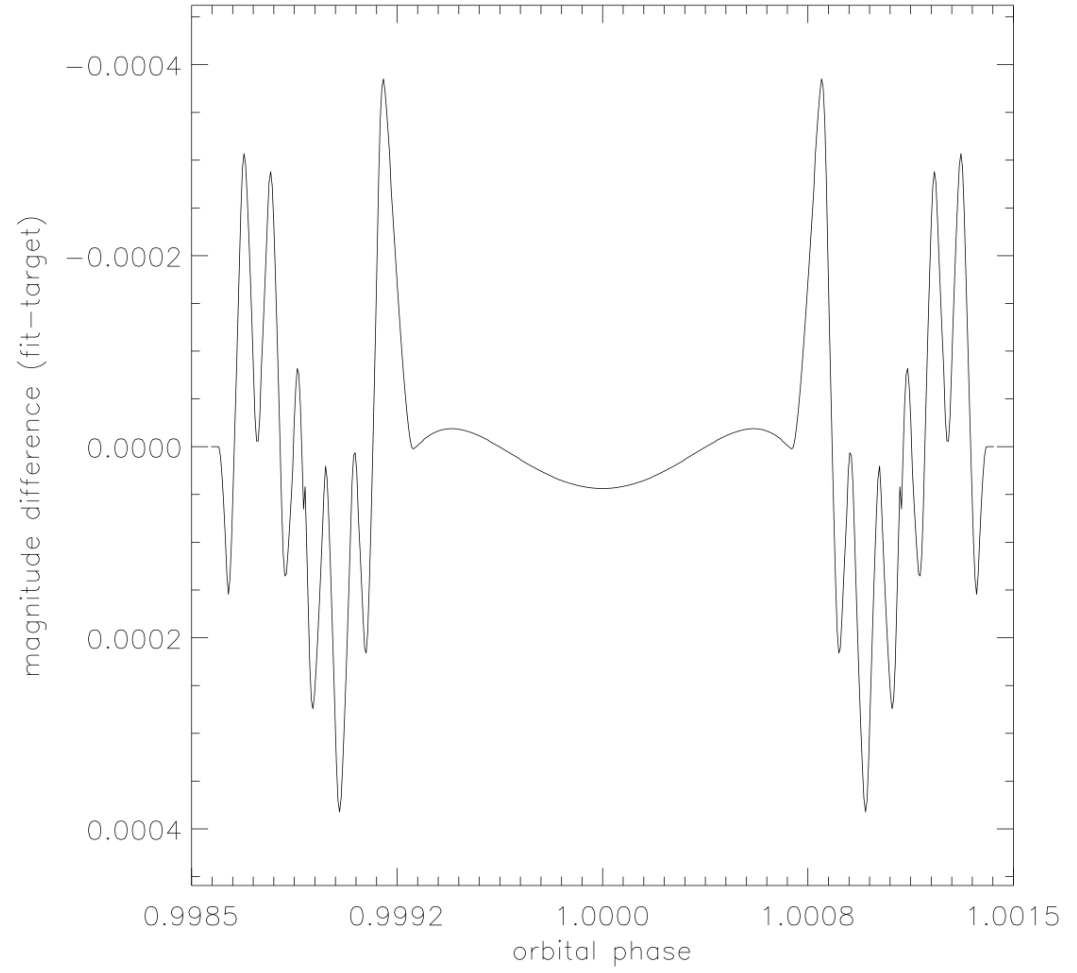


Fig. 1.— Transiting objects: A triangular equilateral object (upper strip) and the spherical planet and star (lower strip, same scale as upper strip). The star mode triangle transit is HD209458 with limb darkening coefficients $u_1 + u_2 = 0.64$ and $u_1 - u_2 = -0.055$ (Brown et al. 2001). The triangle edge length is 0.280 stellar radius. The impact parameter is $b = 0.176$ (transit center). The best-fit sphere has an impact parameter of $b = 0.19$ and a radius of $r_p = 1.16 R_{Jupiter}$. Best-fit star has $u_1 + u_2 = 0$, $u_1 - u_2$ set to zero, and a non-significant radius increase of 0.5%. Fitting object of f , either with zero or 90° obliquity to maintain lightcurve symmetry, converges to f not significantly different from the case $f = 0$.





Looking for an extraterrestrial life?

Ten Anomalies of Transiting Megastructures that Could Distinguish Them from Planets or Stars

Anomaly	Artificial Mechanism	Natural Confounder
Ingress and egress shapes	non-disk aspect of the transiting object or star	exomoons, rings, planetary rotation, gravity and limb darkening, evaporation, limb starspots
Phase curves	phase-dependent aspect from non-spherical shape	clouds, global circulation, weather, variable insolation
Transit bottom shape	time-variable aspect during transit, e.g., changes in shape or orientation	gravity and limb darkening, stellar pro/oblateness, starspots, exomoons, disks
Variable depths	time-variable aspect during transit, e.g., changes in shape or orientation	evaporation, orbital precession, exomoons
Timings/durations	non-gravitational accelerations, co-orbital objects	planet–planet interactions, orbital precession, exomoons
Inferred stellar density	non-gravitational accelerations, co-orbital objects	orbital eccentricity, rings, blends, starspots, planet–planet interactions, very massive planets
Aperiodicity	Swarms	Very large ring systems, large debris fields, clumpy, warped, or precessing disks
Disappearance	Complete obscuration	clumpy, warped, precessing, or circumbinary disks
Achromatic transits	Artifacts could be geometric absorbers	clouds, small-scale heights, blends, limb darkening
Very low mass	Artifacts could be very thin	large debris field, blends

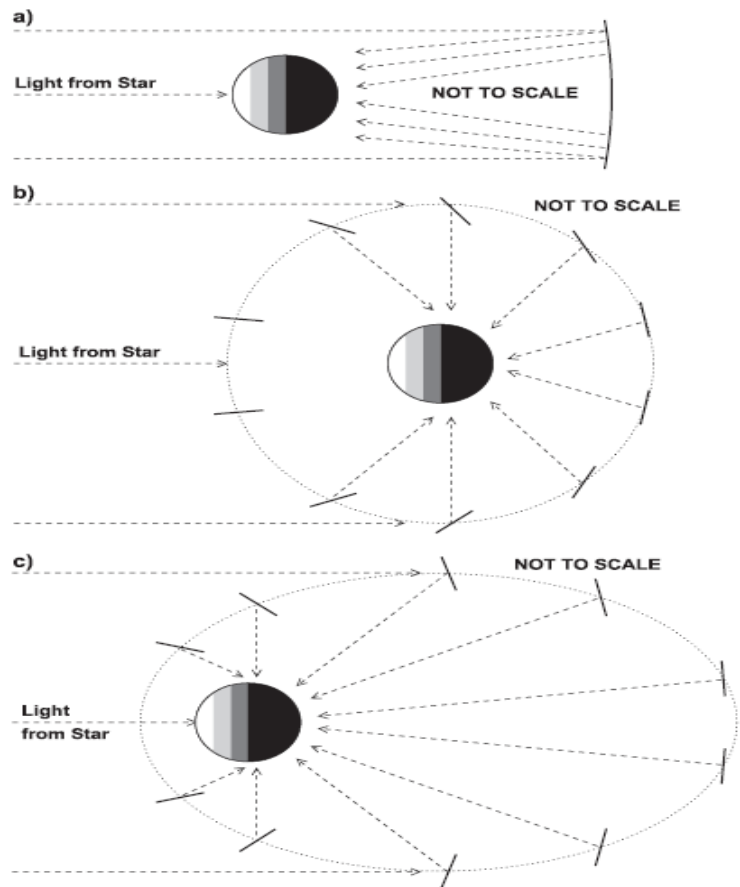


Figure 1. Schematic illustration of three methods of dark-side illumination (not to scale). Planetary grayscale bands indicate different levels in stellar illumination. In the three cross-sectional drawings, (a) shows a large circular or annular mirror stationed at the L2 Lagrange point, (b) shows multiple small mirrors in circular orbits, (c) shows multiple small mirrors in elliptical orbits designed to maximize the duty cycle of the mirrors.

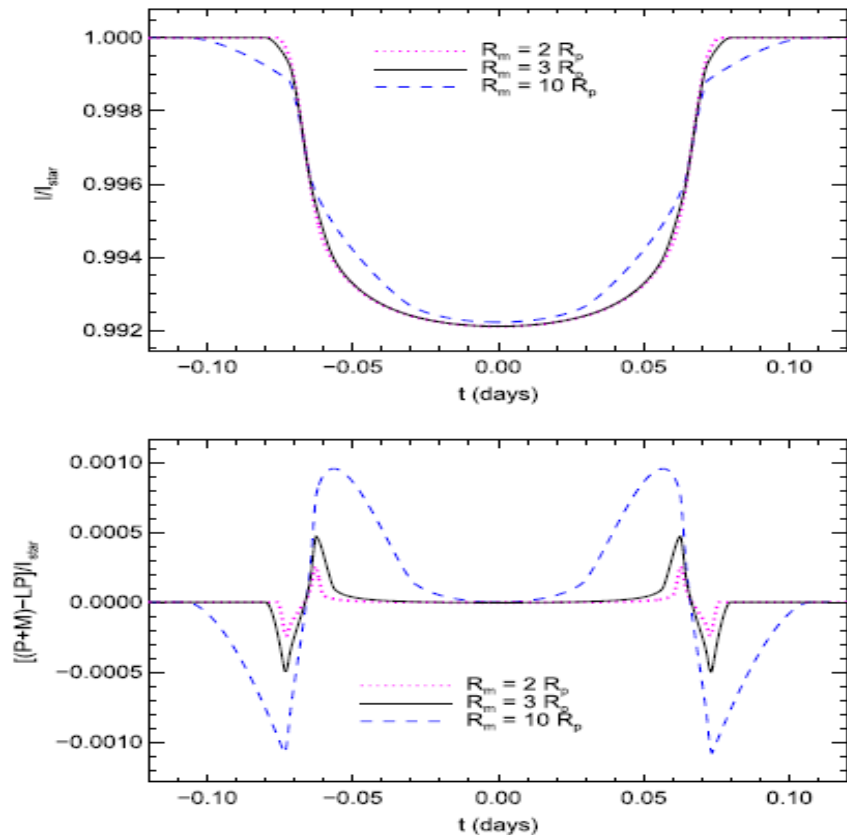
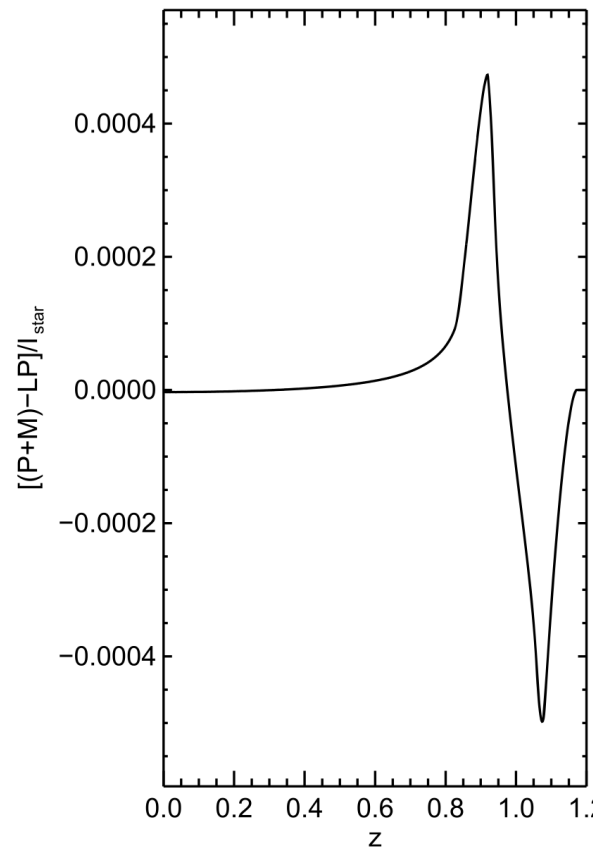
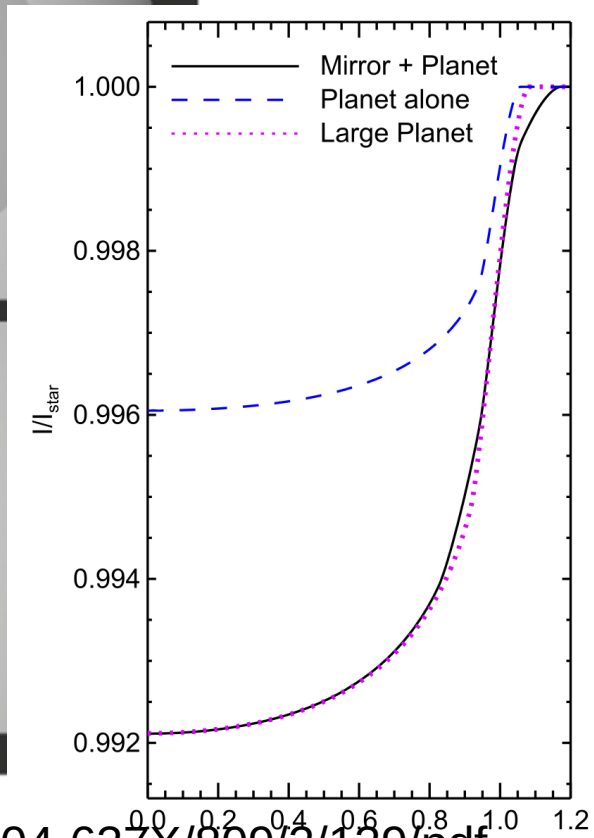
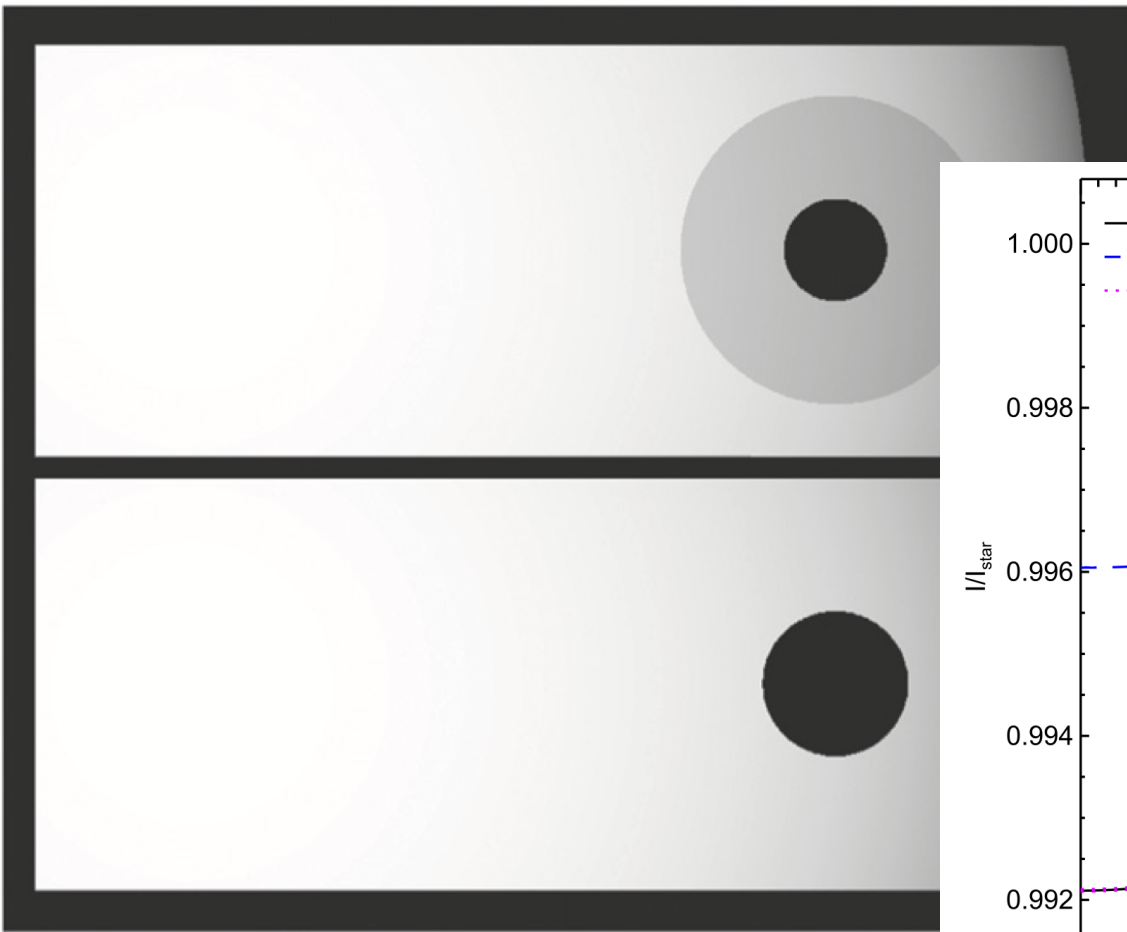
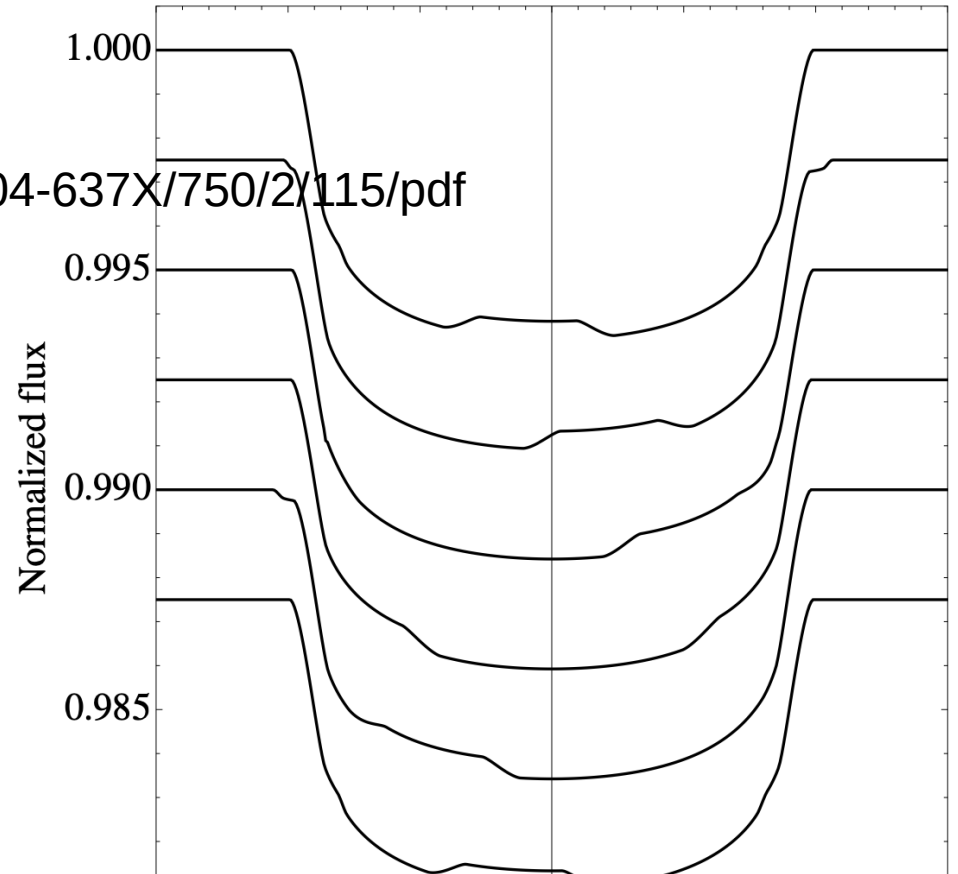
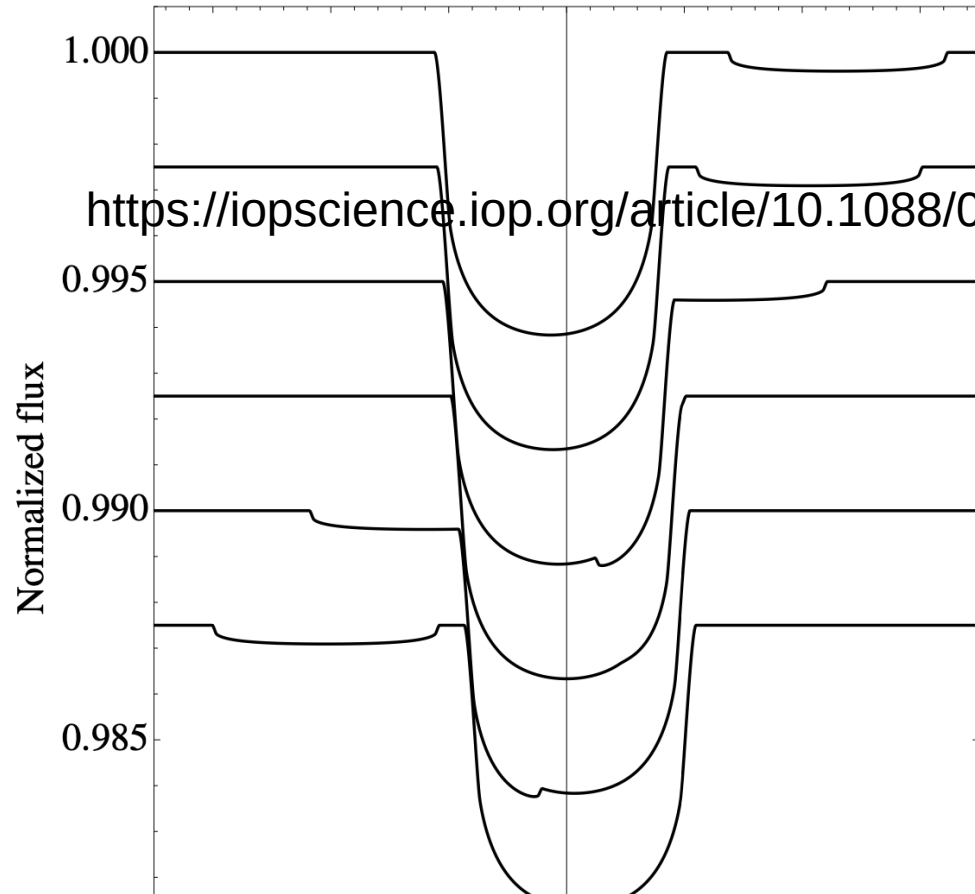


Figure 5. Top panel: transit light curves that result when a planet with $R_p = 2R_{\text{Earth}}$, located in the middle of the star's HZ, passes in front of an M5 star. In all cases the planet is surrounded by a constant-absorptance mirror fleet, with $R_m = 3R_p$ (solid), $R_m = 2R_p$ (dotted), or $R_m = 10R_p$ (dashed). Bottom panel: difference between the mirror fleet transit light curve ($P + M$) and the one for a solitary larger planet (LP) that would produce the same depth of transit, relative to the stellar intensity, for the same situations.

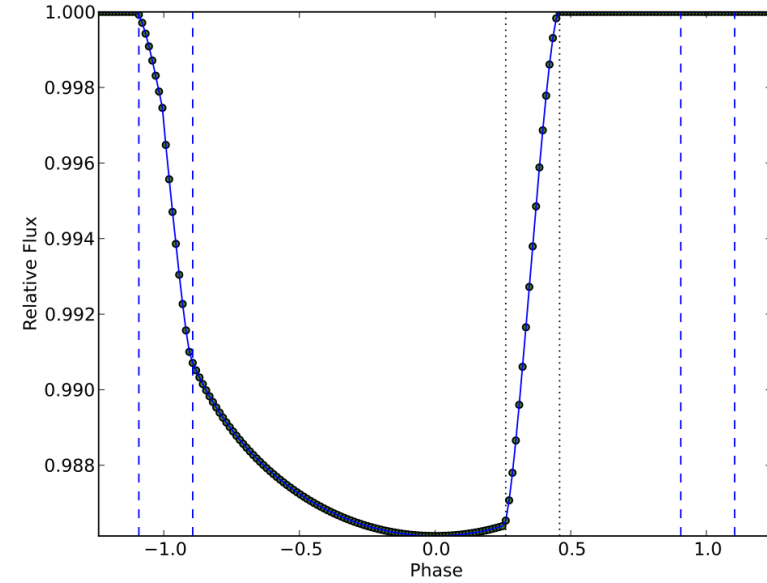
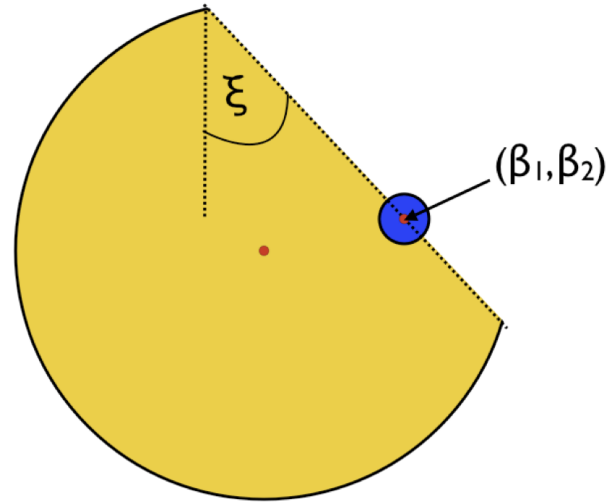
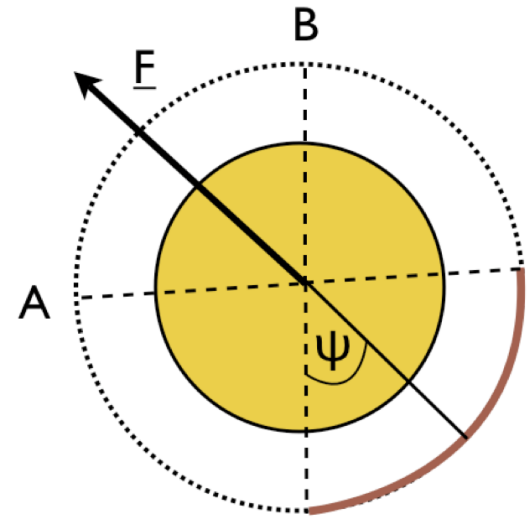


Exo-moons



<https://iopscience.iop.org/article/10.1088/0004-637X/750/2/115/pdf>

Stellar thruster



KIC8462852

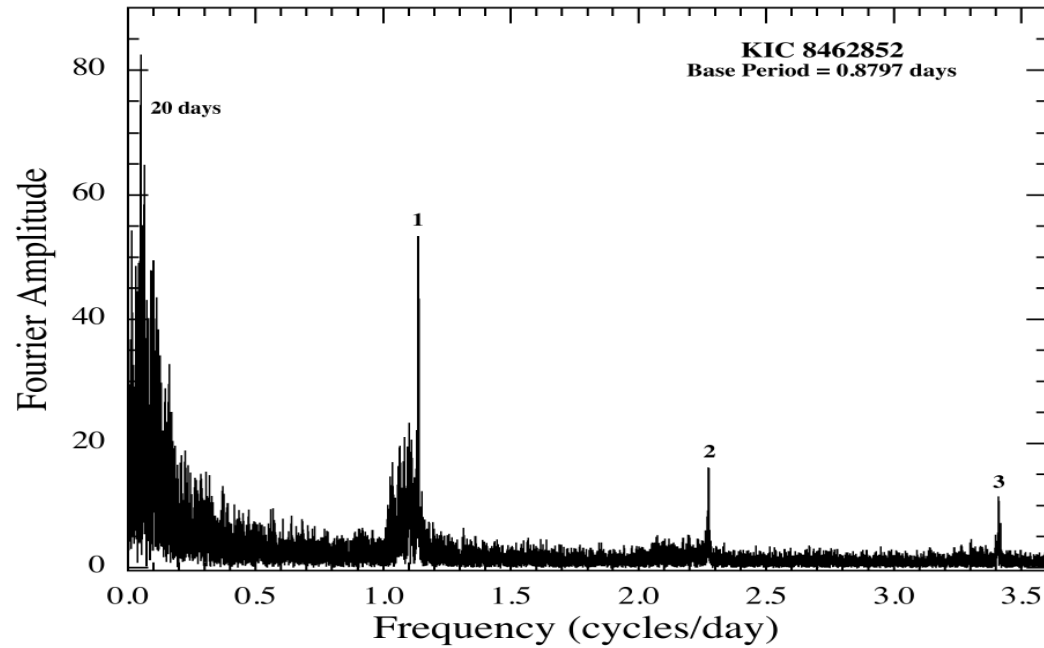


Figure 2. Fourier transform for KIC 8462852. The peaks are labeled with the harmonic numbers starting with 1 for the base frequency. Refer to Section 2.1 for details.

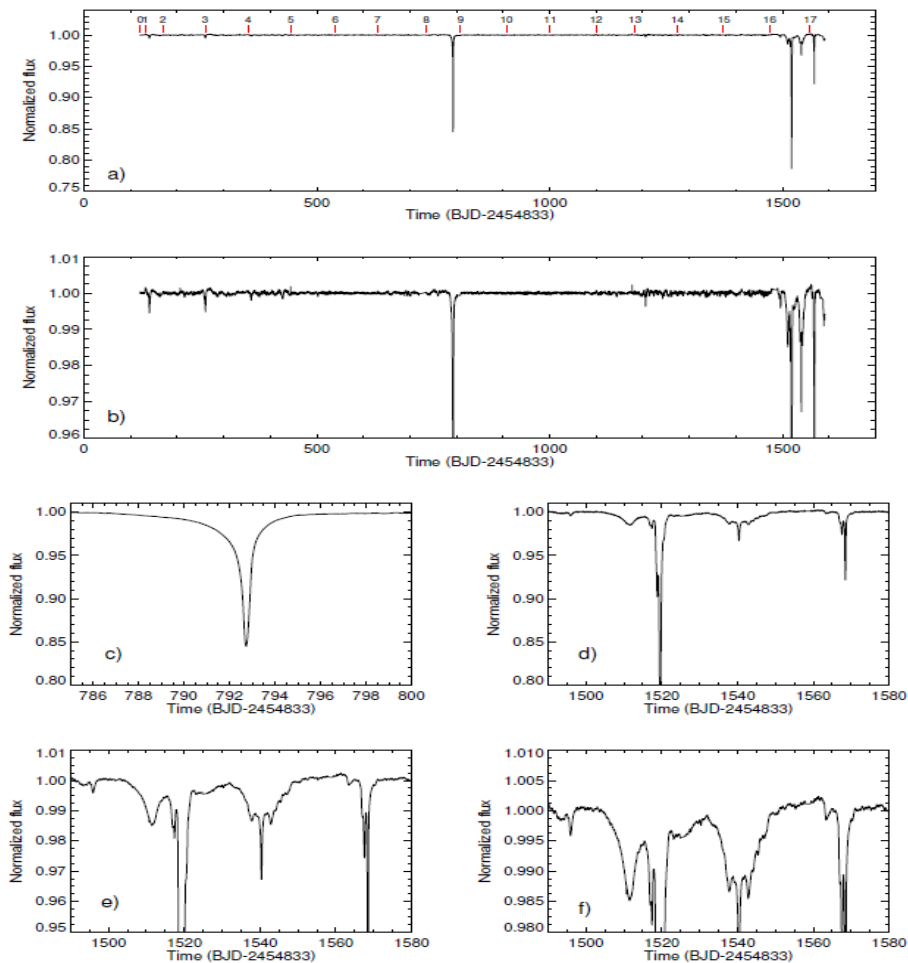


Figure 1. Montage of flux time series for KIC 8462852 showing different portions of the 4-year *Kepler* observations with different vertical scalings. The top two panels show the entire *Kepler* observation time interval. The starting time of each *Kepler* quarter is marked and labeled with a red vertical line in the top panel ‘a’. Panel ‘c’ is a blowup of the dip near day 793, (D800). The remaining three panels, ‘d’, ‘e’, and ‘f’, explore the dips which occur during the 90-day interval from day 1490 to day 1580 (D1500). Refer to Section 2.1 for details. See Section 2.1 for details.

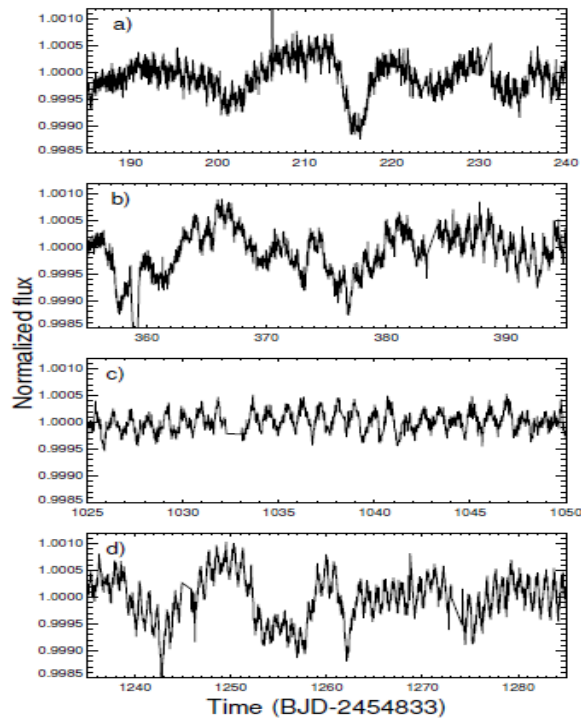


Figure 4. Stacked plots showing a zoomed-in portion of the *Kepler* light curve. The star's rotation period of 0.88 d is seen in each panel as the high-frequency modulation in flux. With the exception of panel 'c', a longer term (10–20 day) brightness variation is observed, also present in the FT shown in Figure 2. Refer to Section 2.1 for details.

tional velocity, and rotation period (Section 2.1), we determine a stellar rotation axis inclination of 68 degrees.

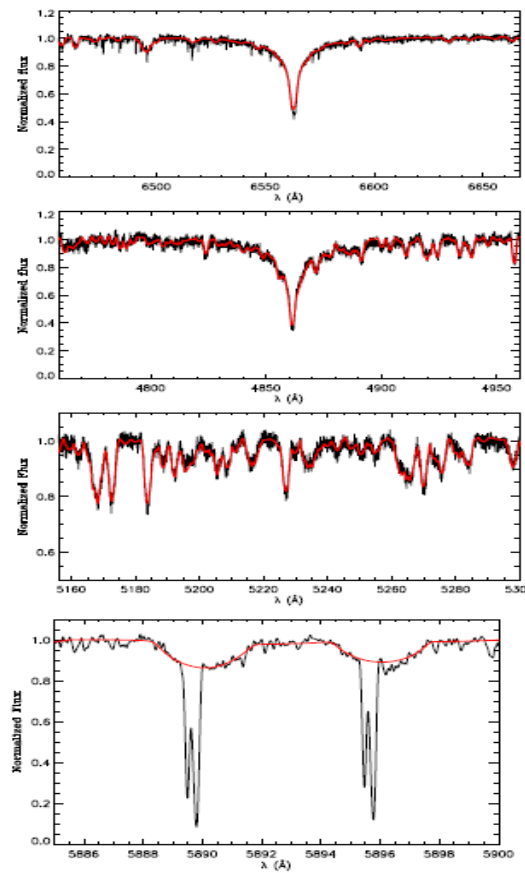


Figure 5. NOT spectrum closeups for KIC 8462852, the best fit stellar model shown in red. Panels show region near $H\alpha$, $H\beta$, Mg, and Na D (top to bottom). The bottom panel shows both the stellar (broad) and interstellar (narrow) counterparts of the Na D lines. Refer to Section 2.2 for details.

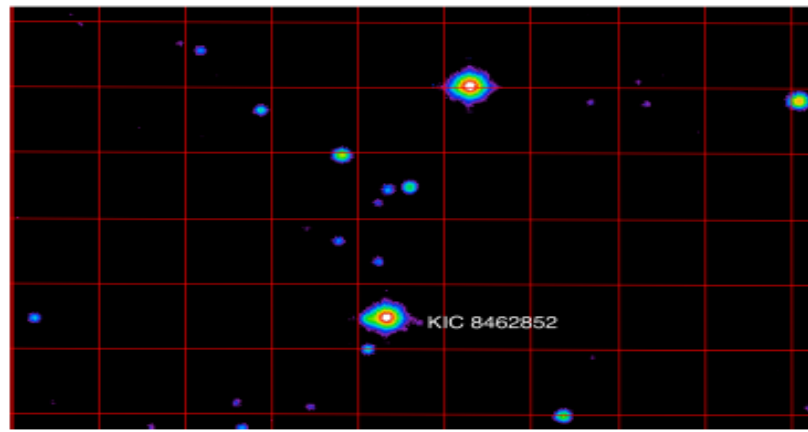


Figure 6. UKIRT image for KIC 8462852 and another bright star for comparison, showing that it has a distinct protrusion to the left (east). For reference, the grid lines in the image are $10'' \times 10''$. Refer to Section 2.3 for details.

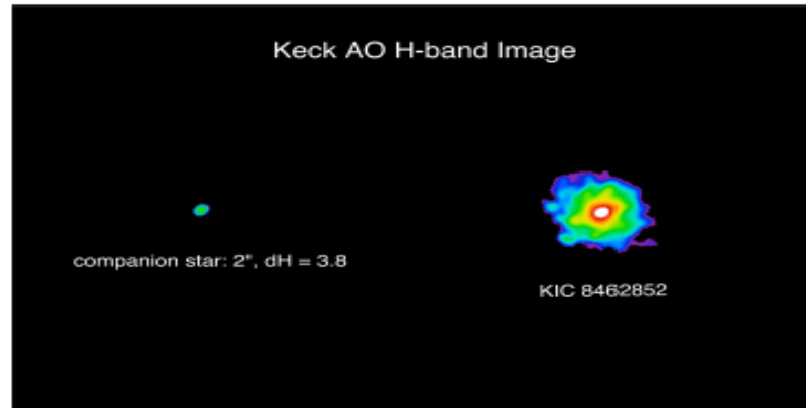
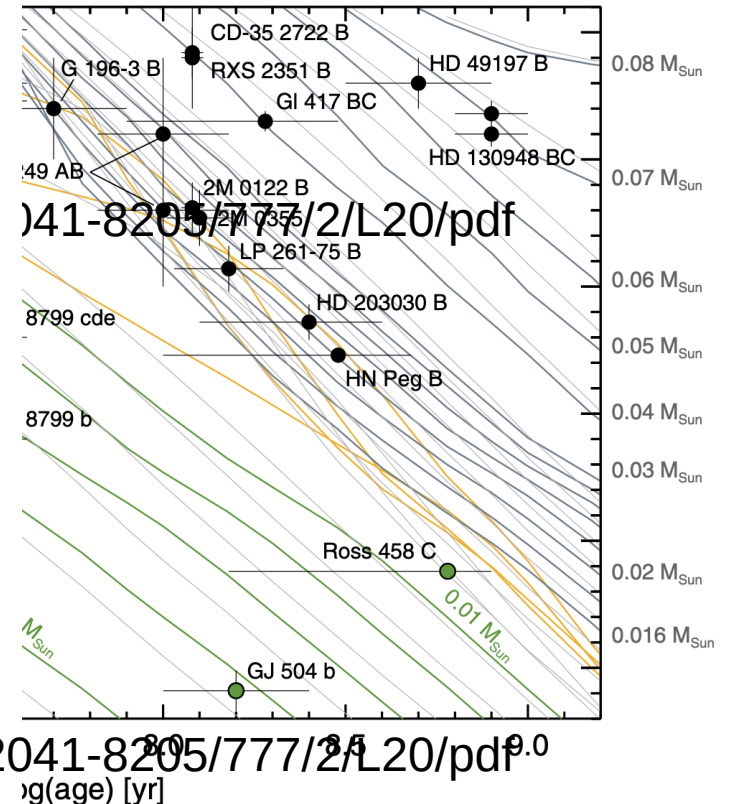
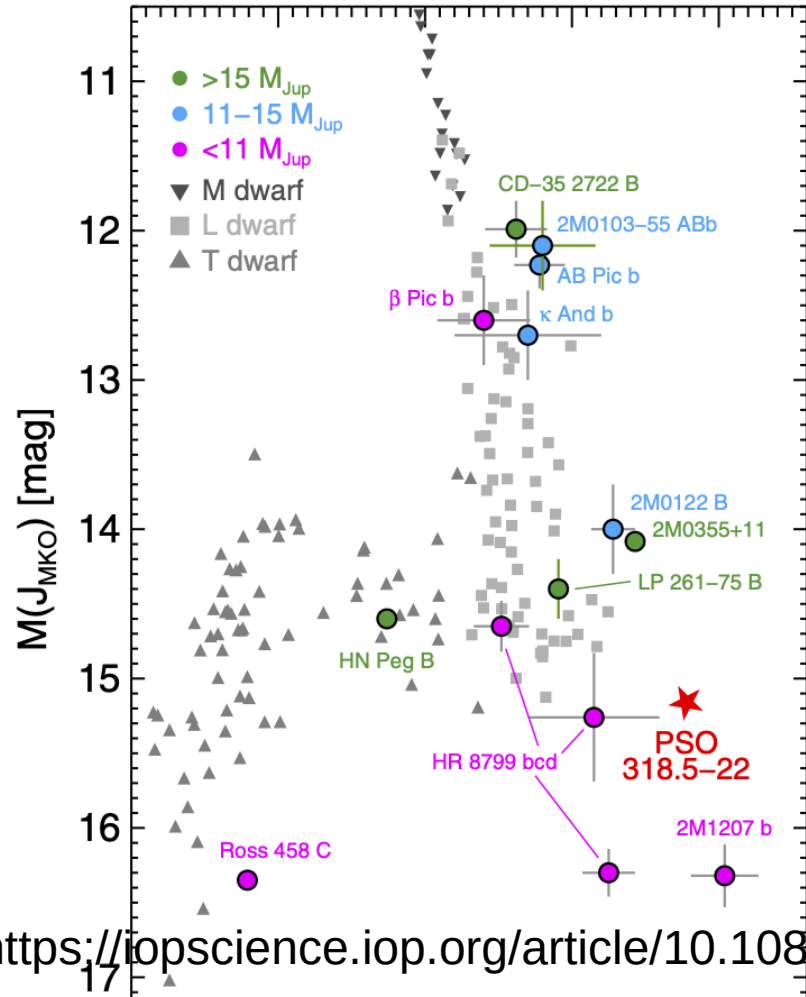
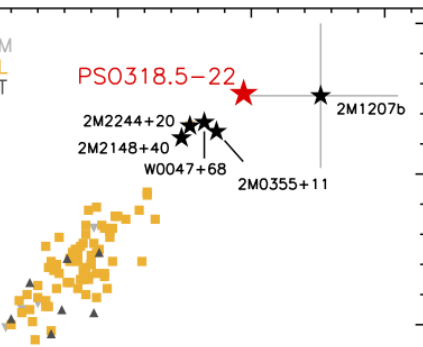
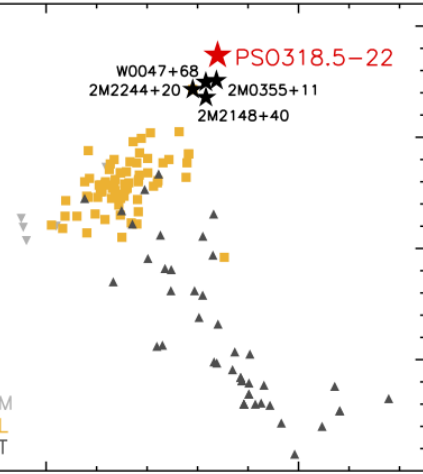


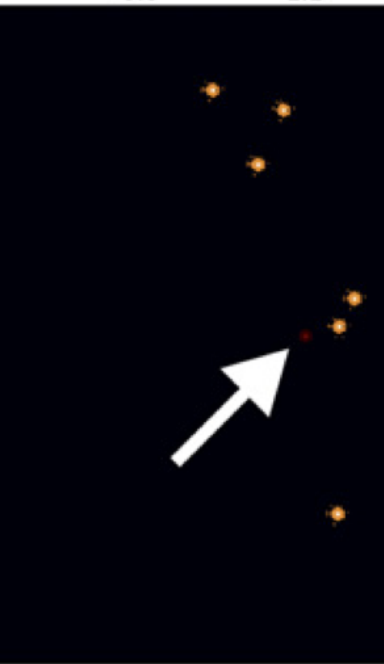
Figure 7. Keck AO H -band image for KIC 8462852 showing the companion was detected with a $2''$ separation and a magnitude difference $\Delta H = 3.8$. Refer to Section 2.3 for details.

Free floating planets

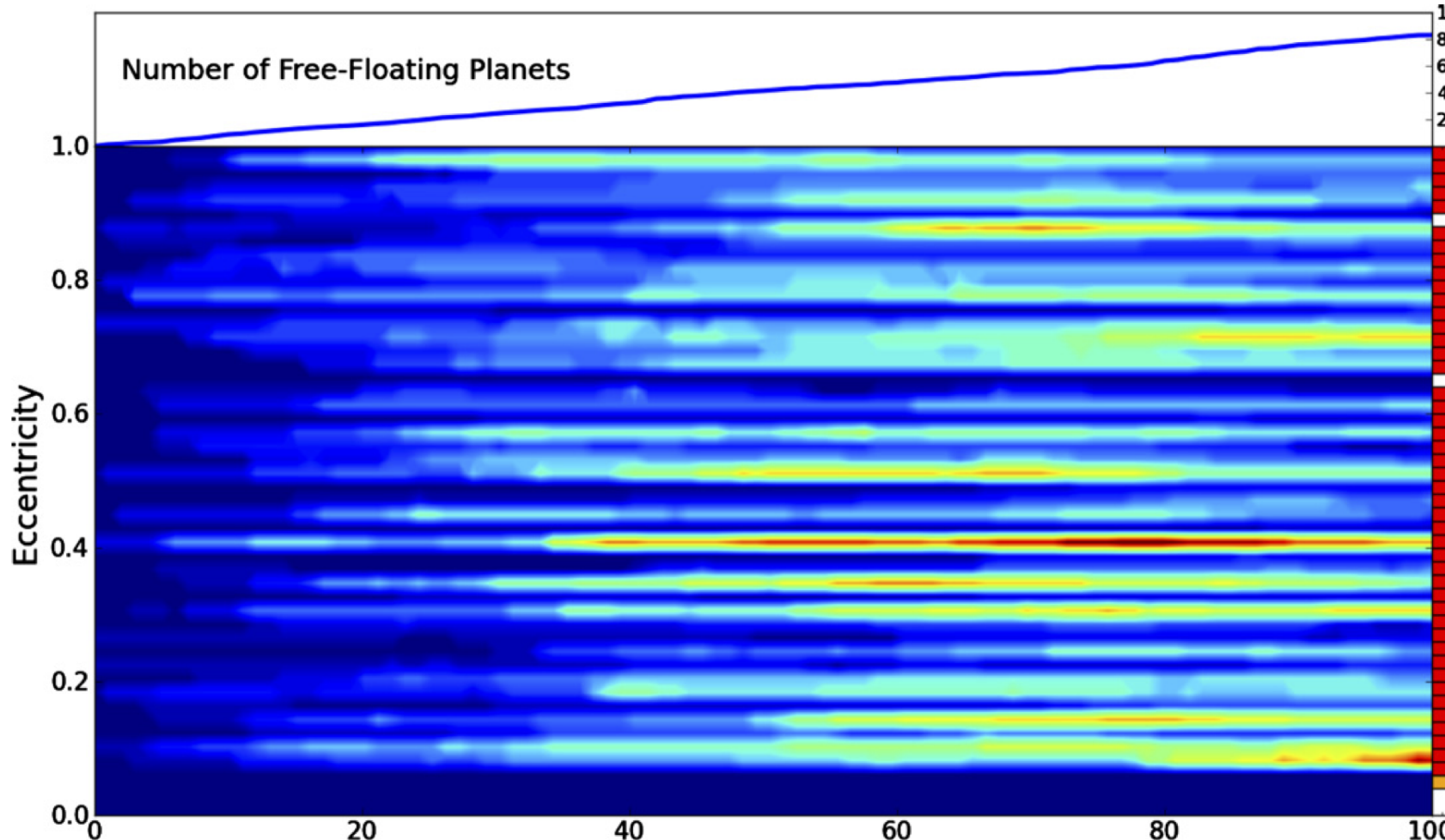


JWST/NIRCam Field of Vi

0.6 1.1

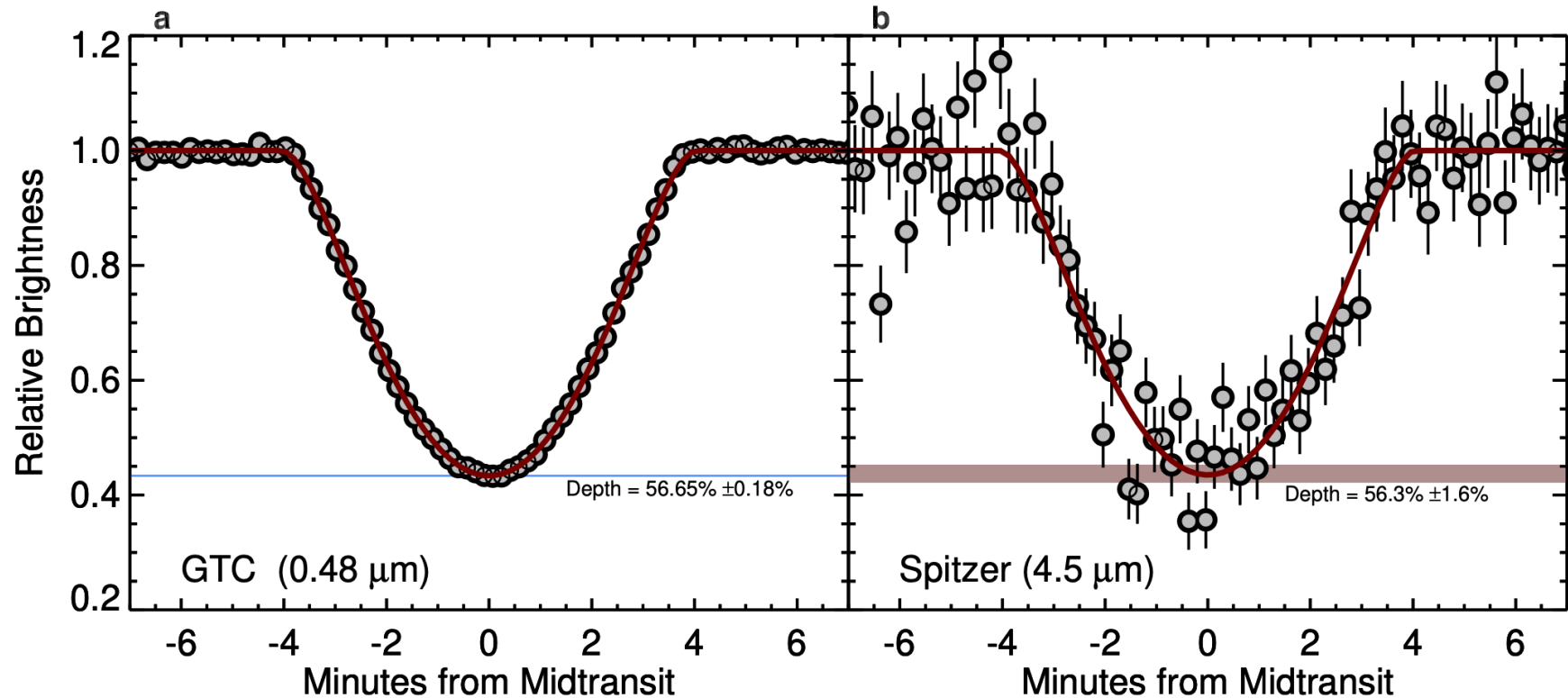


Free-floating plan

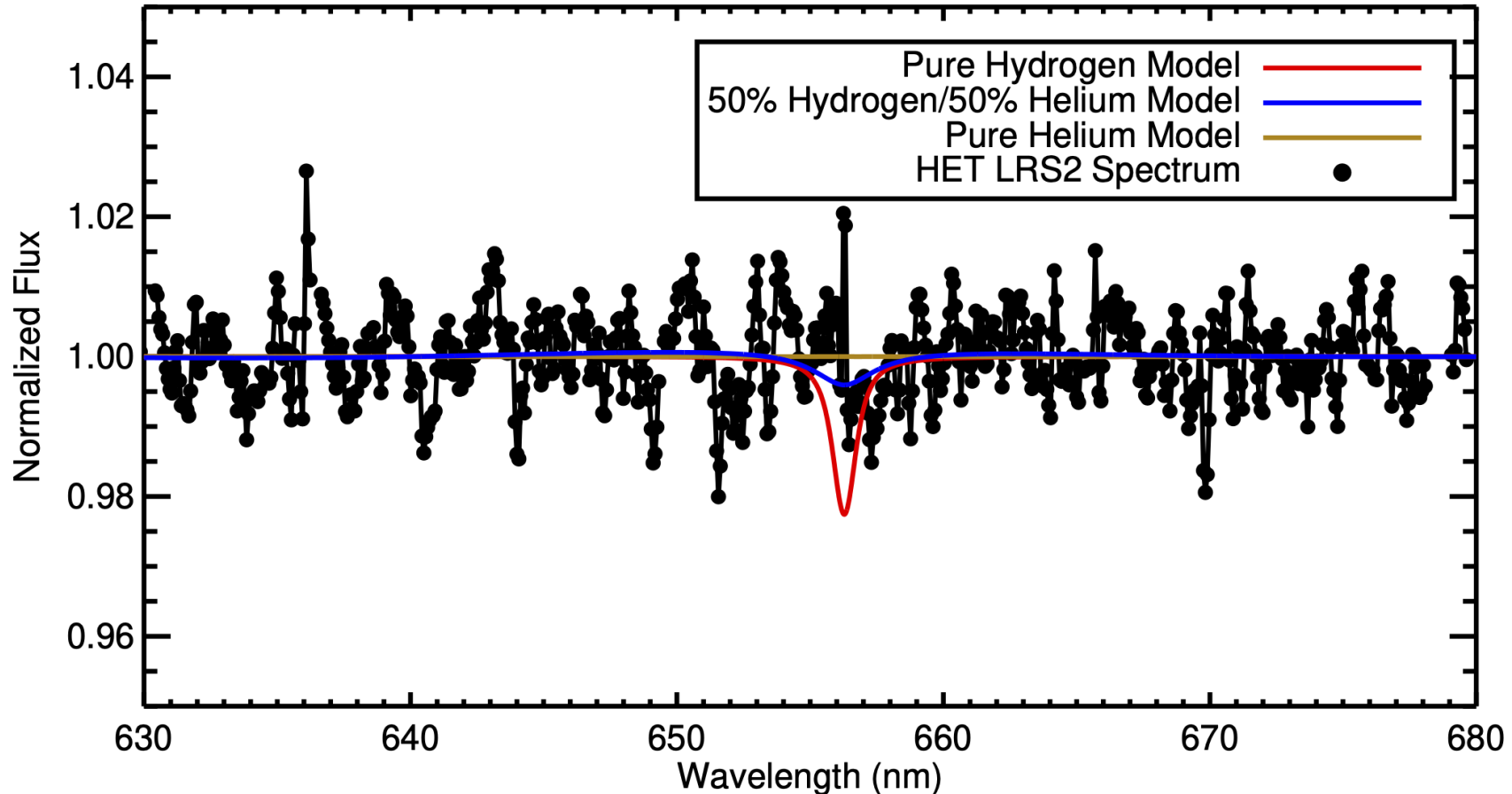


Planets around white dwarfs

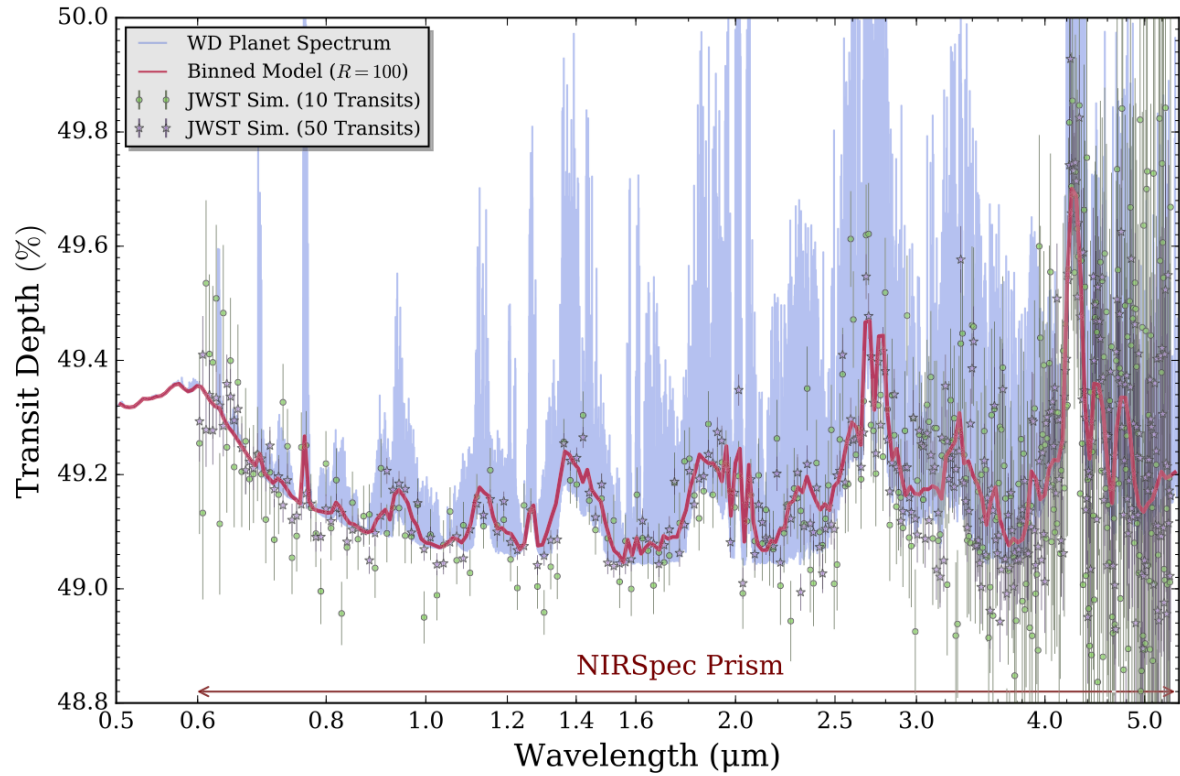
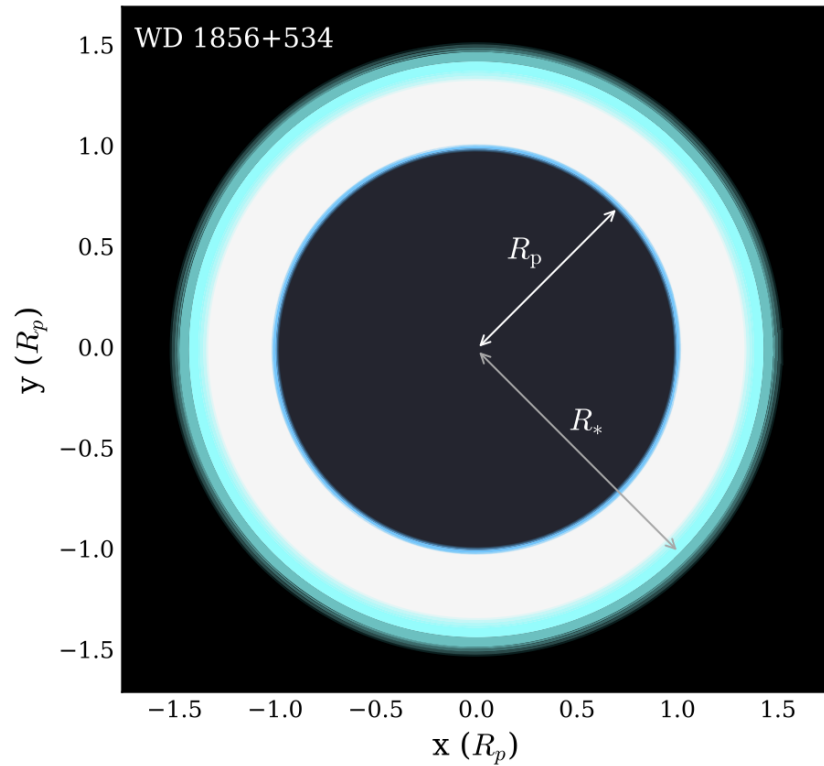
- <https://arxiv.org/abs/2009.07282> - WD1856 detected by TESS



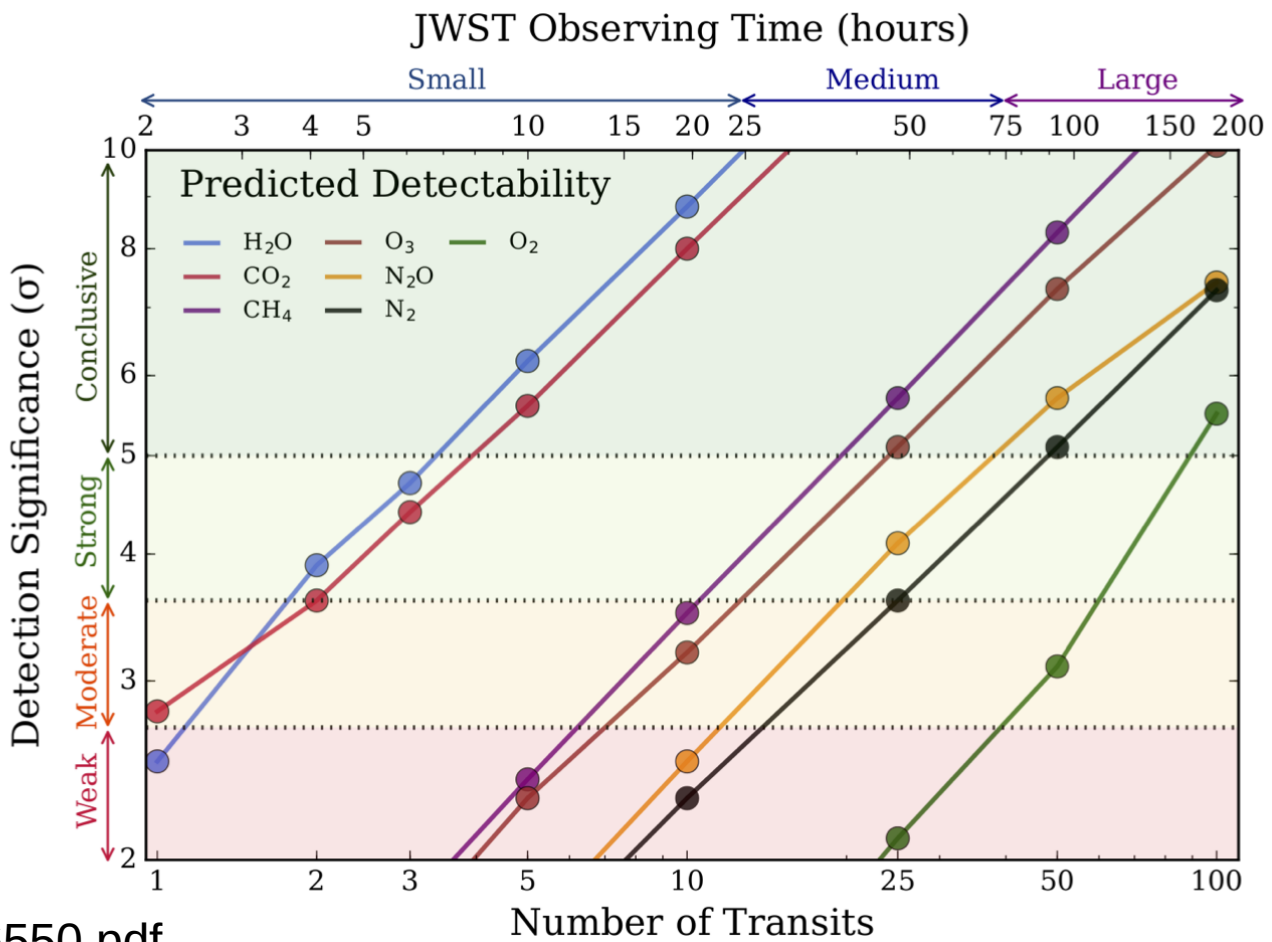
In the HZ?



Why WDs?



Why WD planets?



- Next – future of exoplanetary research and some notes, furthermore, exam topics discussion – DATE TBC

Thank you